ADVANCED INTELLIGENT SYSTEMS Open Access
www.advintellsyst.com

Next-Generation Energy Harvesting and Storage Technologies for Robots Across All Scales

Zexi Liang, Jiarui He, Chuangang Hu, Xiong Pu, Hadi Khani, Liming Dai, Donglei (Emma) Fan,* Arumugam Manthiram,* and Zhong-Lin Wang**

Self-powered untethered robots that can meander unrestrictedly, squeeze into small spaces, and operate in diverse harsh environments have received immense attention in recent years. As there is not a universal solution that can be applied to power robots with diverse forms, service functions, and a broad size range from nanometers to meters, the design, fabrication, and implementation of power systems with a suitable weight, desired power and operation duration, and adaptiveness to confined spaces and operation conditions represent one of the greatest challenges in robotic research. Herein, an overview of recent progress and challenges in developing the next-generation energy harvesting and storage technologies is provided, including direct energy harvesting, energy storage and conversion, and wireless energy transmission for robots across all scales.

1. Introduction

The interest and success in creating robotic machines with diverse functions can be dated back to the Iron Age.[1] Notable examples include the astronomical calculator that displays celestial information made at least 2000 years ago in ancient Greece[2] and the 470-year-old machinery monk that still walks and prays as exhibited in the Smithsonian in Washington, D.C. Nevertheless, only the past half-century has witnessed advanced technologies for underpinning the first commercial robot, Unimate, that replaced the human workforce in transporting and welding giant metal casts in the automobile industry. Since then, diverse robots with distinct appearances, sizes, and functions have been created to perform either often-tedious, high-risk tasks within extreme, human-exclusion environments or those requiring ultrahigh accuracy, speed, and repeatability. Thus far, the impact and potential of robots have been widely extended, ranging from home appliances to manufacturing automation, deep-sea navigation to outer-space exploration,[3] and in vivo-targeted drug delivery to precise medical operation.[4]

In spite of disparate forms, sizes, and functions, all robots possess three essential units that include energy supply, programmable/intelligent control, and mechanical actuation. Suitable design, fabrication, and implementation of the energy unit is pivotal and requires thoughtful consideration of the distinct size, weight, working environment, and power needs of different robots. This consideration is particularly imperative when creating untethered robots, that is, autonomous mobile robots (AMRs) that are self-powered.

Biomolecular machines have powered life for billions of years by harvesting energy from their environments. For instance, nanoscale flagellar motors rotate to propel the locomotion of bacteria cells when seeking food utilizing energy from ionic transportation across cytoplasmic membranes with an efficiency near 100%.[5] Mimicking this mechanism, scientists have developed solar cells to convert solar energy into electricity with an efficiency of up to 30% by leveraging optoelectric properties of semiconductors.[6] Recent innovations in triboelectric nanogenerators (TENGs) have even enabled the conversion of low-frequency mechanical vibrations into electrical energy.[7] Electricity has also been generated from waste heat by harnessing thermoelectric effects.[8] It is imperative to investigate and evaluate innovative schemes and devices that can harness renewable

Z. Liang, J. He, H. Khani, D. Fan, A. Manthiram
Materials Science and Engineering Program and Texas Materials Institute
The University of Texas at Austin
Austin, TX 78712, USA
E-mail: dfan@austin.utexas.edu; rmanth@mail.utexas.edu

Z. Liang, D. Fan, A. Manthiram
Walker Department of Mechanical Engineering
The University of Texas at Austin
Austin, TX 78712, USA

C. Hu, L. Dai
Australian Carbon Materials Centre (A-CMC)
School of Chemical Engineering
University of New South Wales
Sydney, NSW 2052, Australia
E-mail: l.dai@unsw.edu.au

X. Pu, Z.-L. Wang
Beijing Institute of Nanoenergy and Nanosystems
Chinese Academy of Sciences
Beijing 100083, China
E-mail: zhong.wang@mse.gatech.edu

Z.-L. Wang
School of Materials Science and Engineering
Georgia Institute of Technology
Atlanta, GA 30332-0245, USA

The ORCID identification number(s) for the author(s) of this article can be found under https://doi.org/10.1002/aisy.202200045.

DOI: 10.1002/aisy.202200045

energy directly from an environment. Restricted by the temporal and spatial availability of a natural resource, however, renewable energy is generally intermittent and entails a synergized operation with an energy storage system.

Batteries, supercapacitors, and fuel cells are employed ubiquitously to store electric energy or to convert chemical energy into electricity for later use in a gauged manner. These devices are essential in powering diverse forms of robots and underpin the development of superior alternatives to traditional energy technologies. Notably, internal combustion engines that utilize fossil fuels to power conventional vehicles with an energy conversion efficiency of up to 40% are beginning to be replaced by electric vehicles based on batteries, supercapacitors, and/or fuel cells with zero greenhouse gas emission.[9]

Wireless energy transmission is another indispensable scheme for robotic devices that are difficult to be powered due to restricted locations or small sizes. In this regard, short-distance energy transmission by electromagnetic waves has been widely used to supply energy to implanted medical devices.[10] Similarly, multitudes of micro-/nanoscale robots rely on harvesting energy from external physical fields.[11]

While it is difficult to define whether any of the above-powering schemes are more advanced than others, the power demand of a robot is highly sensitive to its specific applications. Particularly, the rapid progress in sea exploration necessitates underwater robots with stable, compact, and high-energy-density storage devices that ensure operation under such extreme conditions. In contrast, the widespread development of drones and aviation vehicles calls for lightweight, high-energy-density, and low-cost energy storage/conversion systems with the ability to withstand robust temperature environments over extended-use periods. Thus, the selection and incorporation of a power/energy source in a robotic system should be considered at an early stage in the primary design as it impacts the rest of the robotic development, that is, working principle, circuit design, weight, size, and packaging. Therefore, we review in this article common measures used for different power systems, including, but not limited to, the size, energy per volume/weight, output power, efficiency, safety, environmental impact, lifetime, and cost. Based on these measures, a suitable single or hybrid power source(s) can be required for a specific robotic system.

Herein, we provide an overview of research and development on the state-of-the-art energy harnessing, storage, and conversion technologies, along with their associated materials, devices, and platforms, required to meet the energy and power demands for AMRs. Although a robot may take myriad forms with dimensions spanning from nanometers to meters, the employed energy scheme is supported generally by one of the three pillar technologies or their combinations, that is, direct energy harvesting and conversion, electrochemical energy storage and conversion, and wireless energy transmission.[12]

2. Energy Harvesting Technologies for Self-Powered Robots

Energy harvesting technologies play a salient role in solving the energy challenges of robots. The renewable energies (such as solar, kinetic, and thermal energies) in the surrounding environments of a robot are free, ubiquitous, and sustainable (**Figure 1**). Ideally, a robot equipped with one or several types of energy harvesting devices could be self-powered with electricity generated from the surrounding renewable energy sources. Therefore, growing interest has been devoted to investigating novel energy harvesting technologies for robots.

3. Solar Cells

Solar energy is readily available outdoors, and our planet Earth receives an annual average solar power of 60≈250 W m^{-2} depending on the location on the Earth.[13] A variety of thin-film photovoltaic devices (or solar cells) has been developed for harvesting the solar energy, aside from dye-sensitized solar cells (DSSCs), where electrolytes are used for charge transport during redox reactions. The solar-to-electrical energy conversion efficiency of solar cells varies with their adopted structures and selected materials. Intrinsically, there are three indispensable components in a photovoltaic device, that is, a cathode, an anode, and a photoactive layer. Generally, the electron–hole pairs are generated by the photoactive layers via absorbing the photoenergy, which are then separated and gathered by the photocathode and anode, respectively. Electron/hole transport materials can be designed to inhibit charge recombination and enhance charge collection in most devices. Depending on the differences in photoactive materials, solar cells can be categorized into many different types. The majority of commercial solar cells utilize silicon as the photoactive material. The efficiency of commercial solar cell panels ranges from ≈8% to ≈30% while utilizing amorphous Si, crystalline Si, or compound semiconductors.[6] Bendable solar cell panels composed of thin-film amorphous Si or copper indium gallium diselenide (CIGS) are already commercially available and can be attached to the curved surfaces of a robot to provide power. In addition, efforts have also been made to develop flexible or even stretchable solar cells, especially for organic solar cells (OSCs) utilizing a photoactive layer composed of the donor material of usually conjugated polymers, conjugated pigments or oligomers, and acceptor materials of usually

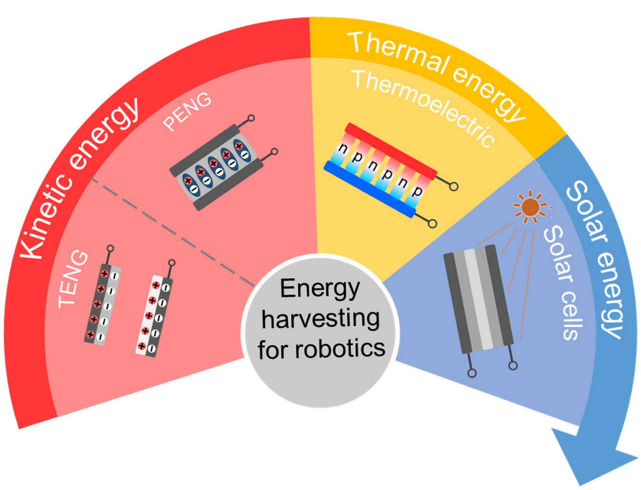

Figure 1. Harvesting renewable energies including kinetic energy, thermal energy, and solar energy for self-powered robots.

fullerene derivatives, perovskite solar cells (PSCs) utilizing perovskite-type organometallic halide as the photoactive materials, and DSSCs utilizing organic dyes to absorb photoenergy with a coupled photoelectrochemical process.[14] A brief summary of materials, performances, and features for various solar cells is provided in **Table 1**.

The same commercially available, unbendable solar panels that successfully integrate with inflexible robots present problems for soft robots, necessitating the development of a flexible solar cell technology. Research on flexible solar cells and self-powered devices has been mainly focused on three types of photovoltaic devices, that is, PSCs, OSCs, and DSSCs (**Figure 2**). All three device types have a strong potential for high flexibility (especially solid-state DSSCs), and each can be processed at ambient temperature with solution-based procedures. However, they all face the challenge of limited long-term stability in ambient conditions or under high temperatures. PSCs possess the greatest potential for high efficiency, with a reported efficiency reaching 25.2%,[15] but flexible PSCs have only been reported to achieve an efficiency of 18.4% and reach a curvature radius of about 4 mm.[16]

Flexible DSSCs have been attempted through strategies using new, transparent conductive electrodes (e.g., metal wire networks[17] and CuS.[18]) and by designing 1D fibers/wires or 2D woven fabrics with integrated DSSCs.[19] A recent work reports a solid–electrolyte-based woven fabric DSSC using a photoelectrode and a counter electrode as weft and warp, respectively.[20] Finally, OSCs suffer from flexibility limitations imposed by the crystalline nature of organic semiconductors, so efforts have been made to improve flexibility by developing all-polymer nonfullerene OSCs. A bending curvature of up to 2 mm has been demonstrated for flexible OSCs[21] and attempts at flexible textile-based OSCs have also been reported.[22] Specifically, two studies report highly deformable OSCs on very thin plastic films (2 μm PET)[23] and elastomer substrates (acrylic elastomer),[24] respectively, where 7.9% efficiency was maintained with 52% stretchability. These highly flexible, deformable solar cells could potentially work as the conformal "skin" or "cloth" of soft robots and serve as power supplies.

Efforts have also been made to integrate solar cells with energy storage devices for self-powered electronics. Solar cells can be connected with energy storage devices through external circuits or using novel structures that have been developed by combining the two devices through shared electrodes, that is, the so-called photobattery or photosupercapacitor.[25] For the former strategy, all three types of solar cells have been attempted[26] and all-fabric-based integrated power systems have been reported wherein fiber-/fabric-based solar cells were combined with energy storage devices.[26b,27] For the latter strategy, dye-sensitized photoelectrodes have simultaneously served as electrochemical electrodes in a battery or a supercapacitor.[19b,28]

4. Triboelectric Nanogenerators

Mechanical motion is ubiquitous and robots themselves also conduct mechanical work. Several technologies exist to convert kinetic energy from mechanical work into electricity, such as the electromagnetic generators (EMGs), piezoelectric nanogenerators (PENGs), and triboelectric nanogenerators (TENGs). The EMG is suitable for large-scale electricity generation from mechanical motions at high frequency, while PENG and TENG are effective for harvesting energy from mechanical motions at low frequency and amplitude.[29] Another advantage of the two kinds of nanogenerators is the potential in realizing flexible or wearable devices. The PENG was first introduced in 2006 using ZnO nanowires for harvesting tiny mechanical energies.[30] The state-of-the-art progresses can be found in the recent reviews.[31] Here, we will only focus on the TENG, as the PENG is applied in very similar situations as the TENG but the TENG shows higher output and better multifunctionalities. In particular, the TENG can be intrinsically flexible as it only requires conductive and dielectric thin-film materials. Low modulus, high stretchability, or self-healing capability can be readily achieved using correspondingly elastomeric polymer materials.[32] The mechanical-to-electrical conversion of the TENG is based on the coupled effect of contact electrification and electrostatic induction, leading to its high-voltage output characteristic. Therefore, it can serve as a high-voltage source to power

Table 1. Comparison of several different types of solar cells.

Type	Typical active materials	PCE [%]	Advantages	Disadvantages
DSSCs	Ruthenium polypyridyl dye, alcian blue, aniline blue, bromophenol blue, methyl orange, beetroot, Henna leaves, cocktail dye	4.5–14.3[49,50]	Low cost Efficient in weak light conditions Flexibility	Low efficiency Liquid electrolytes
PSCs	$MAPbI_3$, $FAPbI_3$, $MAPbBr_3$, $MAPbCl_3$, $CsPbI_3$, $CsPbBr_3$, $MAPbI_xBr_{3-x}$, $Cs_2AgBiBr_6$, $Cs_2AgInCl_6$	3.8–24.3[46b,30]	High efficiency Low cost High power/weight ratio	Environmental sensitivity Limited mechanical robustness Pb is toxic
OSCs	$PC_{61}BM$, P3HT, PTB1, PTB7-Th, PDBT-T1, PBDTTT-E-T, PBDTTT-C-T	2.9–18.7[47b,31]	Roll-to-roll synthesis Light weight Good flexibility	Relatively low efficiency Relatively short lifetime
Silicon solar cell	Amorphous Si, crystalline Si	8–26.1[47a]	High efficiency High reliability Long lifetime	Limited flexibility High density

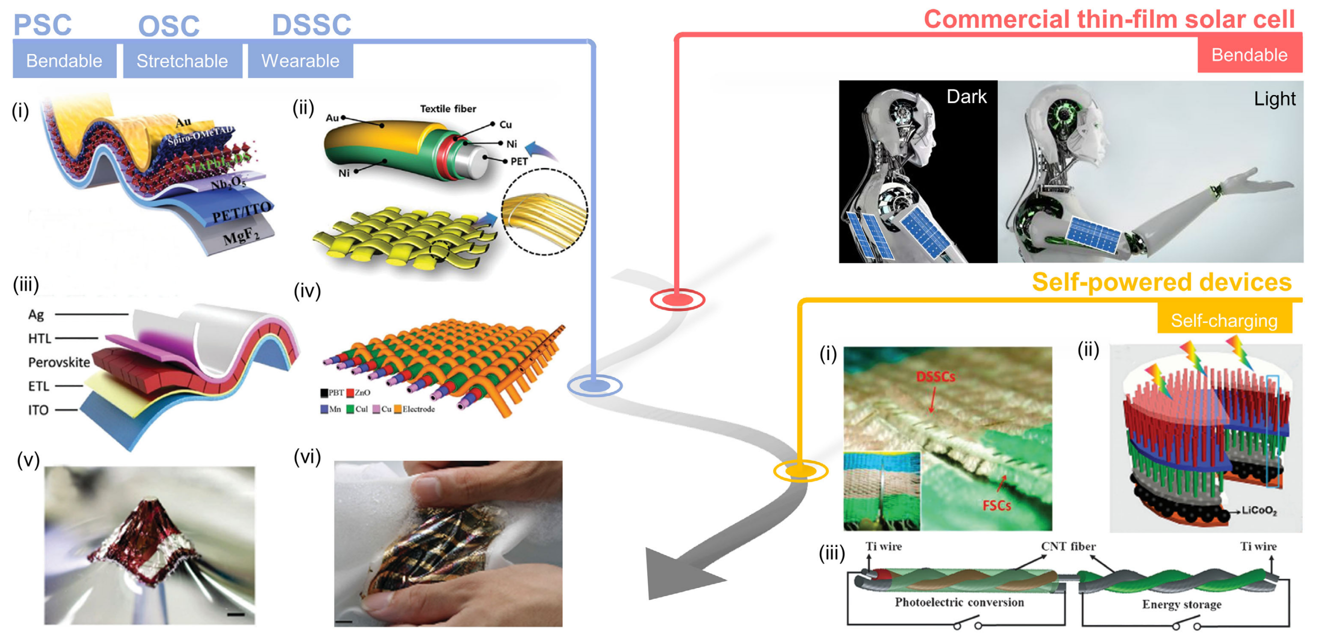

Figure 2. Left: Wearable solar cells for robots. Bendable commercial thin-film solar cells could be the "cloth" or "skin" of a robot. Bendable, stretchable, or wearable PSCs, OSCs, and DSSCs are being further studied, such as i) a bendable PSC (Reproduced with permission.[16] Copyright 2018, Wiley), ii) a fiber-shaped OSC (Reproduced with permission.[35f] Copyright 2014, Elsevier), iii) a bendable PSC (Reproduced with permission.[7] Copyright 2016, Wiley), Copyright 2016, Wiley), iv) a textile DSSC (Reproduced with permission.[20] Copyright 2016, Wiley), and v and vi) stretchable polymer solar cells. (Reproduced with permission.[23] Copyright 2012, Springer Nature; (Reproduced with permission.[24] Copyright 2017, Springer Nature). Right: Self-powered devices are also being explored by integrating solar cells with energy storage devices, such as i) a self-charging textile with fiber DSSCs and supercapacitors (Reproduced with permission.[26b] Copyright 2016, American Chemical Society), ii) a self-charging photobattery (Reproduced with permission.[28] Copyright 2012, American Chemical Society), and iii) a fiber device with both solar cells and an energy storage unit (Reproduced with permission.[19b] Copyright 2012, Wiley).

electrically responsive soft actuators or as a self-powered sensor for robot–human interfaces.[33] These merits make the TENG a highly promising power device for soft robots. TENG uses Maxwell's displacement current as a driving force for converting mechanical energy/triggering into electric power/signal.[34] A TENG can perform three types of functions in a soft robot, as shown in **Figure 3**. First, it can be a power source to drive the sensors or actuators of a robot. Two approaches have been developed for this purpose. In the first approach, the electricity generated by a TENG can be stored in energy storage devices (either batteries or supercapacitors) with the aid of a conditioning circuit to maximize the power utilization efficiency. The integrated energy system is called the self-charging power system (SCPS), and the stored energy can be supplied to robotic electronics continuously or intermittently.[35] A variety of sensors or wearable electronics have been demonstrated to be intermittently powered by the SCPS with a simple rectifying circuit or be continuously driven by the SCPS with an impedance-matching management circuit. Wireless communications have also been powered for data transfer or remote controls. Considering the versatility of the TENG in structure designs and material selections, the technology has been designed to work in the form of fibers, fabrics, thin films, balls, or 3D architectures and has shown exceptional multifunctionalities, including stretchability, transparency, biocompatibility, biodegradability, implanting ability, and self-healing capability.[32,36] In the second approach, the TENG can serve directly as a high-voltage power source to drive actuators or soft robots.[33] For example, a TENG has been employed to drive electrically responsive dielectric elastomers;[37] to power piezoelectric microactuators or micromotors;[38] and to serve as electrostatic actuators for manipulating the motion of tiny objects, small water drops, and microfluidics.[39]

TENG technology can also serve as a self-powered sensor for soft robots. The mechanical-to-electrical conversion in a TENG itself is a transducer that allow robots to perceive the surrounding mechanical signals (e.g., stress, strain, and vibration)[40] and to function as a robot–human interface for remote control or virtual reality (VR)/augmented reality (AR).[41] The following examples showcase the sensory capabilities of TENG technology: a self-powered auditory sensor that has been developed based on a TENG for use as an electronic auditory system for robotic applications;[42] self-powered triboelectric angle sensors with nanoradian resolution reported for use in robotic arms and personal healthcare;[43] a triboelectric soft robotic skin that can actively sense proximity, contact, and pressure to external stimuli;[44] TENG-based micromotion sensors that can sense the motion of blinking eyes for applications in human–robot interactions;[45] textile-based triboelectric sensors for human–robot interaction or VR/AR applications;[41,46] flexible TENG-based tactile or contactless sensors for robotic electronic skins;[47] and soft robots using self-powered TENG configurational sensors.[48]

In prospect of the commercialization of TENG in robotic systems, following challenges are still required for further investigations.[49] As a power source, the output power of the SCPS system has to be further improved. This requires future studies on the optimization of TENG generators and the design of an

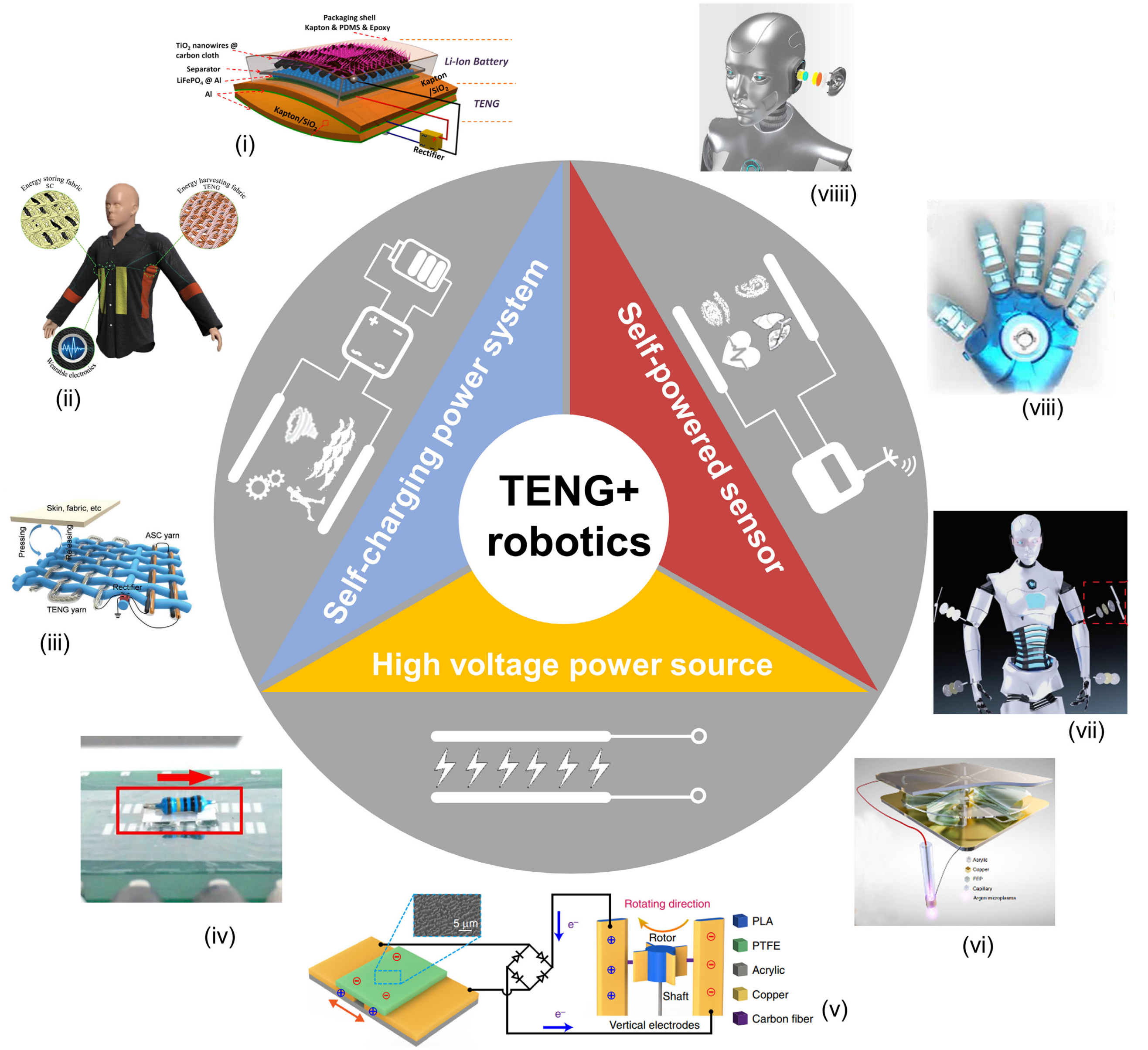

Figure 3. The application of TENGs in robots. The SCPS, such as i) a TENG integrated with a battery,[35e] ii) a self-charging power textile,[35a] and iii) fiber-shaped TENG integrated with fiber supercapacitors.[35d] The TENG as a high-voltage power source iv) to manipulate the motion of small objects,[39c] v) to power a micromotor,[38b] and vi) to excite microplasma.[39d] The TENG as self-powered sensors for robots, such as vii) a triboelectric angle sensor for robots,[43] viii) a smart glove for AR/VR,[41] and viiii) a self-powered auditory sensor.[41] i) Reproduced with permission.[35e] Copyright 2013, American Chemical Society; ii) Reproduced with permission.[35a] Copyright 2016, Wiley; iii) Reproduced with permission.[35d] Copyright 2013, Wiley; iv) Reproduced with permission.[39c] Copyright 2018, American Chemical Society; v) Reproduced with permission.[38d] Copyright 2019, Springer Nature; vi) Reproduced with permission.[39d] Copyright 2018, Springer Nature; vii) Reproduced with permission.[43] Copyright 2013, Wiley; viii) Reproduced with permission.[41] Copyright 2013, AAAS.

appropriate power management circuit, as the high-performance SCPS demands high-output TENG and the minimized impedance mismatch between TENG and its energy storage unit. Recent studies showed exciting progresses, but further demonstration in robotic systems at different levels of power consumption still requires systematic studies.[50] As a self-powered sensor or robotic interaction interface, the current progresses suggest exciting potentials, but future studies may be needed to evaluate the advantages over competing technologies and to stabilize the technical routes for better device reproducibility/durability.

5. Thermoelectric Generator

Thermal energy is another well-known renewable, environmental energy source, particularly the low-grade thermal energy that originates from small temperature differences between nearby objects. This has given rise to the development of thermal technologies like thermoelectric generators, that contain no moving parts and can be miniaturized. A thermoelectric generator typically contains both *p*-type and n-type semiconductors that are electrically connected in series but thermally connected in parallel. The *zT* value is the figure-of-merit parameter of a thermoelectric material. Currently, efforts have been extensively made to develop flexible/wearable thermoelectric generators using conventional inorganic thermoelectric materials (e.g., Bi_2Te_3 and Sb_2Te_3),[51] 2D materials,[52] and organic thermoelectric materials (e.g., PEDOT:PSS and PEDOT:Tos).[53] These signs of progress have been summarized in several recent review papers.[54] Furthermore, several self-powered sensors or electronic devices based on thermoelectric generators have also been demonstrated.[55] For example, a wearable thermoelectric generator with output power around 13–38 $\mu W\ cm^{-2}$ from body heat can provide energy continuously for an electrocardiography system;[55a] a flexible thin-film thermoelectric generator is also reported to harvest body heat and provide power for a pressure sensor;[56] other than human body heat, a 272 mW thermoelectric generator, harvesting heat energy from a 70 °C heat pipe, is reported to power wireless monitoring of temperature, humidity, CO_2, and organic compound concentrations.[57] As for robotic applications, it is important to find appropriate conditions where heat sources are available and heat gradient is high in the future studies. By far, most of the reported self-powering demonstrations are based on human body heat for wearable applications, and the output power also requires further significant improvement.

6. Energy Storage Technologies for Robots

6.1. Batteries

Currently, batteries, which are classified into primary (nonrechargeable) batteries or secondary (rechargeable) batteries, are still the main power supplies for robotic systems. Inexpensive primary batteries, such as alkaline batteries, are suitable only for certain applications. Currently, commercially available secondary batteries, such as lead-acid, nickel–metal hydride (NiMH), and lithium-ion batteries (LIBs), utilize several different battery chemistries for their operation. Lead-acid batteries show several appealing properties, such as low cost, a wide range of operating temperatures, and simple charging protocols. This makes them very attractive and places them as the largest market share of secondary batteries in the world. The poor performance, low gravimetric energy density, and limited lifespan of lead-acid batteries impose significant challenges to their application in small portable electronics. Until recent developments, NiMH batteries remained the potential for AMRs. The reactions in NiMH batteries rely on hydrogen ion-absorbing porous metal alloys and are distinct from those involved in other competing battery chemistries. Owing to its unique reaction, the NiMH systems show several advantages, including low internal resistance, long cycle life, and fast recharging capabilities. However, when compared with LIBs, NiMH batteries also present some disadvantages, such as a limited operating temperature range, a moderate memory effect, higher cost, and lower specific power. These drawbacks led to a gradual displacement of NiMH batteries by LIBs in most applications. LIBs, which utilize Li ions (Li^+) to transport charge between the cathode and the anode, have shown a great potential as a rechargeable energy storage device owing to their high energy density. As illustrated in **Figure 4**A, an LIB mainly includes three parts: a Li-ion intercalation anode, a Li-ion intercalation cathode, and a separator soaked with a Li-ion-conducting electrolyte.[58] The reaction mechanisms of LIBs rely on the intercalation and deintercalation of Li ions, in which Li ions transfer between the anode and the cathode during the charge and discharge processes. In a typical LIB, the anode mainly consists of carbonaceous materials such as graphite that show a low Li intercalation potential and low volume change. Although graphite has a theoretical specific capacity of 372 $mAh\ g^{-1}$, which is only 9% of lithium metal (3860 $mA\ h\ g^{-1}$), it exhibits good stability and prolonged lifespan.[59] The most commonly used cathode materials for commercial Li-ion batteries are layered lithium nickel manganese cobalt oxides (NMC), olivine lithium iron phosphate, and spinel lithium manganese oxide. The electrolytes for conventional LIBs are mainly prepared by dissolving a lithium salt, such as lithium hexafluoro-phosphate, in organic solvents, like diethyl

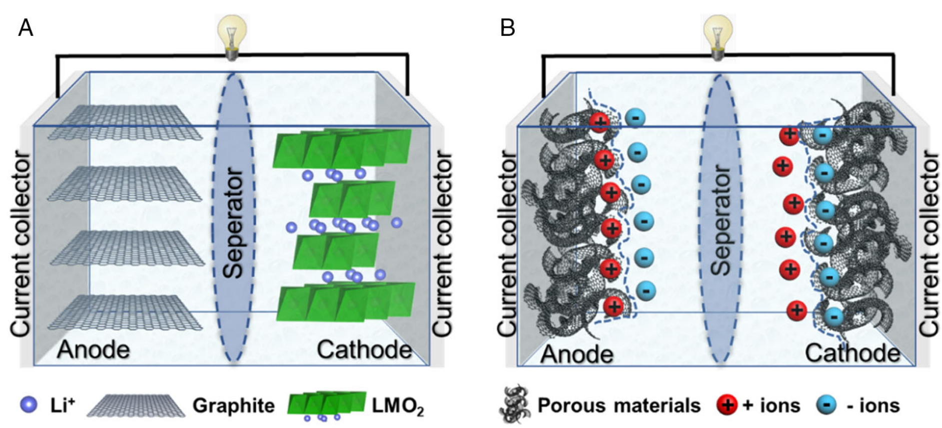

Figure 4. A) Schematic description of a "(lithium-ion) rocking chair" cell that employs graphitic carbon as anode and a transition metal oxide as cathode. B) A scheme of a symmetric supercapacitor.

carbonate, ethylene carbonate, dimethyl carbonate, or mixture of these solvents.

In recent years, the market of LIBs has increased substantially, especially in portable electronics and electric vehicles. LIBs offer high energy densities, approaching those of alkaline primary batteries and higher than those of most commercial rechargeable batteries. More importantly, LIBs have excellent low-temperature performance, high charge retention, high cell voltages, and long lifespan. In particular, layered oxide cathodes with a high nickel content demonstrate a high energy density and long cycle life.[60] These systems exhibit great potential in rechargeable batteries. Currently, most battery technologies are focused on liquid electrolytes owing to their high ionic conductivity and good wettability of the active material. However, the safety problems associated with the flammable organic liquid electrolytes usually pose a challenge to their application. In particular, physical damage to the device or overcharging of the cells can result in thermal runaway, venting, fire, and even explosion. Furthermore, the capacity of liquid electrolyte batteries is also permanently affected by the limitations in the cutoff charge and discharge voltages. In this regard, the monitoring of individual cells in the pack is essential. Advanced battery systems based on solid-state electrolytes are regarded as a promising strategy for realizing future lithium-metal batteries and are being widely investigated. These batteries can ensure a high level of reliability and safety by electronically and physically separating the lithium-metal anode from the cathode while avoiding self-discharge and short-circuiting.

Beyond the current commercially available rechargeable batteries, there has been an intense investigation of sodium-ion, metal–sulfur (including lithium–sulfur, Li–S), and metal–oxygen batteries, which provide greatly improved energy density at a low cost.[61] The practical application of Li–S batteries has already been demonstrated by a prototype of the High Altitude Pseudo-Satellite aircraft of Airbus Defense and Space, which was powered by solar energy during the day and by Li–S batteries at night under realistic conditions during an 11-day flight.

Here, we note that although lithium-based batteries, owing to their high energy density and lightweight, are considered as a promising energy storage system for various applications for now, mining lithium can cause resource problems and political issues in the future, so alternatives such as sodium-ion or sodium–sulfur batteries are under consideration and investigation as we move forward.

Redox flow batteries have attracted intensive development as alternative energy storage technologies and are well known for their excellent scalability, flexible modular design, active thermal management, and better security.[62] Previously, the low power and energy density of flow batteries make them unsuitable for small-scale applications, although they are still a good option for large-scale energy storage. Until recently, miniaturized redox flow batteries have enabled an electrolytic vascular system for an untethered aquatic soft robot.[63] In addition to these developments in advanced battery technologies, the advent of supercapacitors, which showcase larger capacities than conventional electrostatic capacitors and higher charge/discharge rate capabilities than primary/secondary batteries, provides new opportunities for deployment of high-power energy storage devices; the drawback is their lower energy density compared with that of batteries.

Stretchable and soft batteries with high energy densities are recently gaining much interest for wearable electronics,[64] but their applications in soft robotic devices have not been widely recognized thus far. For example, Wirthl et al.[64a] fabricated a stretchable battery in which a tough and stretchable hydrogel electrolyte is sandwiched between the anode (Zn) and the cathode (MnO_2) pastes. The proposed hydrogel demonstrates a self-healing characteristic (i.e., interfacial polymerization of cyanoacrylate monomer) that enables instant tough bonding between the hydrogel components of the anode, separator, and cathode, which substantially reduces the internal resistance and increases the specific capacity ($\approx$1.6 mA h cm^{-2}). Wang et al.[65] developed biomimetic aramid nanofiber-based composites with desired mechanical and ion transport properties as ion-conducting membranes. Such membranes with cartilage-like nanoscale morphology enable pliable zinc–air batteries with conformal shape that can be integrated on the robot body.

6.2. Supercapacitors

Supercapacitors are based on electrostatic or Faradaic electrochemical processes. As shown in Figure 4B, a supercapacitor consists of a pair of electrodes with highly porous surfaces, such as activated amorphous carbons, metal oxides, or conductive polymers.[66] Typically, the cathode and anode are separated by an ion-permeable separator soaked with an electrolyte.

Generally, supercapacitors can be classified into two types: electric-double-layer capacitors (EDLCs) and electrochemical pseudocapacitors (EPCs). The general charge storage mechanism of EDLCs is similar to that of conventional capacitors in which the charge is mainly stored through rapid adsorption−desorption of electrolyte ions at the interface of electrodes and electrolyte by the electrostatic interaction derived from the polarization of the pair of electrodes. The capacitance of EPCs is based on the fast and reversible Faradaic redox reactions occurring near the surface of the electroactive materials. By incorporating pseudocapacitive (i.e., redox active) materials with fast Faradaic reactions and an ultrahigh surface area, supercapacitors can deliver much higher specific capacitance and energy density compared with those of conventional capacitors. Owing to their unique charge storage mechanism, supercapacitors show fast charge and discharge rates within seconds or minutes, which is much faster than that of batteries. In addition, the high-power-density supercapacitors are environmentally friendly, offer excellent safety, and can be operated over a wide temperature range with an ultralong lifespan. More importantly, because of the feasibility to endow stretchability via strategical materials selection and structural design,[67] which offers the feasibility to work ideally under different environments and to combine with other units to build an integrated wearable robotic system, stretchable supercapacitors also show great potential as a main power source.

Particularly, pseudocapacitors based on redox reactions of active electrode materials (as well as metal–air/CO_2 batteries (vide infra)) overcome the challenges associated with low energy and power density of EDLCs[68] and LIBs,[69] respectively;[68b,70]

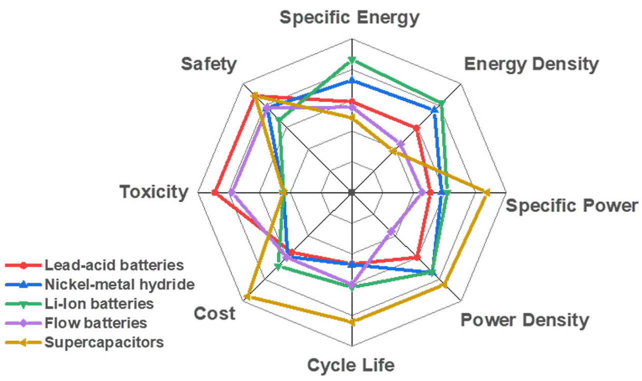

Figure 5. Performance comparison of lead-acid, NiMH, LIBs, and flow batteries along with supercapacitors; values were taken from other studies[73a,b].

they provide high energy/power densities and have attracted a great deal of interest.[68a,71] According to the aforementioned advantages, indeed, supercapacitors show great potential for applications in communications, transportation, electronics, aviation, to name a few. Examples include their use as uninterruptible power supplies (backup supplies to protect against power disruption) and load levelers (backup power for memories, microcomputers, clocks, and system boards).[72] The key characteristics of these five main types of energy storage devices are compared in **Figure 5** and **Table 2**.[73]

6.3. Integrated Energy Systems for Robots

Renewable energy technologies provide attractive power sources for autonomous robots with reduced size, reduced weight, and long endurance as important mission parameters (**Figure 6**). The successful integration of robots with renewable energy requires integrated energy systems as a viable power source that can be stored and generated. In this section, we present a focused review of hydrogen fuel generation (via solar-powered water splitting) and storage for fuel cell technology given that most other renewable energy technologies have been discussed earlier.

Robots used as drones, autonomous vehicles, and submarines (particularly underwater and deep-sea exploration) with large sizes are intrinsically energy intensive and require a stable, high-energy-density power supply for long-term operation.[12] With a high energy density from highly efficient energy conversion, polymer–electrolyte–membrane fuel cells (PEMFCs) deliver higher gravimetric and volumetric energy densities compared with batteries, which are required for powering the robots with long-duration missions.[74] Instead of burning fuel to generate electricity and waste heat, fuel cells convert chemical energy directly into electricity by oxidizing hydrogen at the anode and reducing oxygen gas at the cathode with water as the only byproduct.[75] Because of its high energy conversion efficiency (40–60%, or up to 85% efficiency if waste heat is captured for use), minimal pollution, and great potential for large-scale applications, fuel cell technology currently receives intensive research and development focus.[75,76] Compared with conventional batteries, such as lead-acid and NiMH (Figure 6), one of the big advantages of fuel cells is their ability to decouple energy storage from power production, which provides power continuously for long-duration missions so long as fuel (e.g., hydrogen fuel) is supplied. This makes fuel cells attractive for mobile robots that always demand higher energy storage (Figure 6). With no major moving parts, low maintenance needs, and easy integration into large stacks, hydrogen fuel cells can provide an extremely high energy density to ensure long endurance of large robots in land, water (deep sea), and space(https://www.toyota.com/mirai/fcv.html).[12,77] Fuel cells offer the additional advantage of quiet operation (i.e., without noise and/or vibration), making them attractive power sources for reliable operation in precision robots[78] (Figure 6). However, the slow oxygen reduction reaction (ORR) at the cathode is a key step to limiting the energy conversion efficiency of a fuel cell and requires a substantial amount of platinum catalyst (representing at least one-quarter of the fuel cell cost). This, together with the requirement for safe hydrogen storage, has limited fuel cell technology for widespread commercial adoption.

Hydrogen can be stored, transported, and consumed without emission of any greenhouse gas byproduct[79] and offers multiple advantages over traditional fossil fuels (Figure 6), such as a higher energy content per unit weight compared with all fuels (52 000 Btu lb^{-1}, three times greater than that of gasoline)[80] and a high theoretical usable energy density for compressed hydrogen [≈120 MJ kg^{-1} (6–9 MJ kg^{-1} practical), around 86 times of that of LIBs (1.40 MJ kg^{-1} theoretical,

Table 2. Characteristics of five key types of energy storage devices.

Characteristics[a)]	Lead-acid batteries	NiMH batteries	LIBs	Flow batteries	Supercapacitors
Specific energy [Wh Kg^{-1}]	30–50	60–120	170–300	10–50	0.07–85.6
Energy density [KWh m^{-3}]	60–110	140–300	350–700	10–33	1–35
Specific power [W Kg^{-1}]	25–415	6–1100	8–2000	31.3–166	5.4–100 000
Power density [KW m^{-3}]	10–400	7.8–588	56.8–800	2.5–33.4	15–4500
Cycle life [cycles]	100–2,000	300–3,000	250–10 000	800–16 000	10 000–1 000 000
Cost [USA$ KWh^{-1}]	50–1,100	200–729	200–4000	100–2000	100–94 000
Toxicity	High	Low	Low	Moderate	Low
Safety	High	Moderate	Moderate	Moderate	High

a)Values are taken from Ref. [73a,b].

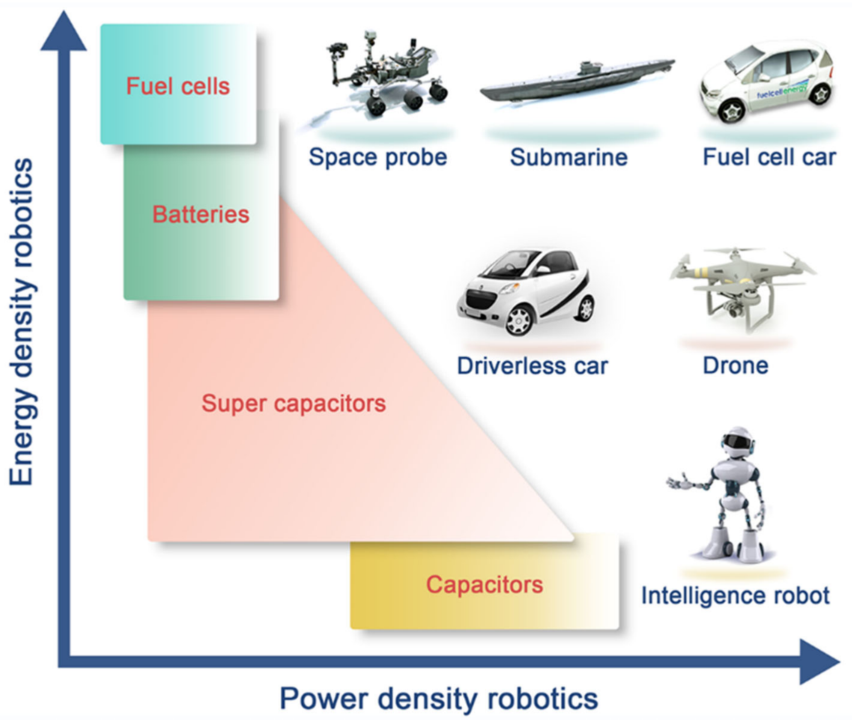

Figure 6. Simplified Ragone plot of the energy storage domains for various renewable energy technologies useful for specific robots.

0.36–0.47 MJ kg^{-1} practical)].[81] Electrocatalytic water splitting, driven by renewable energy (such as solar, wind, hydropower, and even tribogenerator), has been widely viewed as a promising strategy to produce H_2 gas[82] for hydrogen fuel cells. Hence, integration of fuel cells and water splitting technologies holds great promise for generating clean electricity from water and sunlight (vide infra). However, efficient water splitting requires expensive precious metal-based catalysts (e.g., Pt, RuO_2, IrO_2) with limited resources to promote the hydrogen evolution reaction (HER) and oxygen evolution reaction (OER).[32a,83] In addition to the ORR in fuel cells, Pt has also been demonstrated to be very efficient for the HER in acidic electrolytes, while Ir- and Ru-based precious metal oxides are highly active toward the OER in alkaline electrolytes.[71] This electrolyte mismatch for the HER and OER catalysts, together with the high cost of precious metal-based catalysts, has prevented the overall water splitting and its integration with fuel cell(s) from commercial applications.[35a,84]

To date, considerable effort has been made to substitute precious metal-based catalysts with nonprecious-metal catalysts that have already been demonstrated to be viable in alkaline hydrogen fuel cells.[85] Although the precious metal volume can be reduced by this approach, nonprecious metal catalysts are still too expensive for commercialization of renewable technologies and present efficiency issues. Along with intensive research efforts to develop promising nonprecious metal catalysts, a new class of carbon-based metal-free electrocatalysts (C-MFECs) has been discovered to be effective for the ORR, OER, and HER.[86] Subsequent studies showed that C-MFECs exhibited improved durability and catalytic performance compared with state-of-the-art nonprecious metal catalysts for the ORR even in acidic PEMFCs [87] and that multifunctional catalytic activities can be achieved for various electrocatalytic reactions, such as the ORR and OER in Zn–air batteries;[88] the OER and HER in water-splitting units;[89] and the ORR, OER, and HER in integrated energy systems consisting of an electrocatalytic water-splitting unit powered by on-board PSCs that produce O_2 and H_2 gases with which fuel cells can generate clean electricity.[84] In fact, the combination of a hydrogen fuel cell with a water-splitting electrolyzer driven by solar energy (**Figure 7**) has been used to power mobile robots and new-age cars.[80,90]

To ensure robots have a stable and long operating time, an additional hydrogen storage tank is often needed to provide a constant and continuous supply of H_2 gas to the fuel cell (Figure 7). Being the lightest gas in the atmosphere, however, hydrogen storage requires a large space. Therefore, an attractive option to store hydrogen efficiently as a portable power source for robots is to compress H_2 gas into a pressurized cylinder or liquidize it at a low temperature (below −253 °C). However, whether it is stored under compression or in liquid form, hydrogen presents downsides, including unavoidable leakage and risk of explosion during transportation and/or operation. To overcome these limitations, metal alloys and certain solid-state metal hydrides (e.g., $LaNi_5H$, PdH_x) that safely absorb large amounts of H_2 reversibly under desired temperatures and pressures have been developed for efficient hydrogen storage; they can even store twice the amount of hydrogen allowed by liquid hydrogen in containers of the same volume or one thousand times its original gas form.[91] Although a group of Mg-based hydride

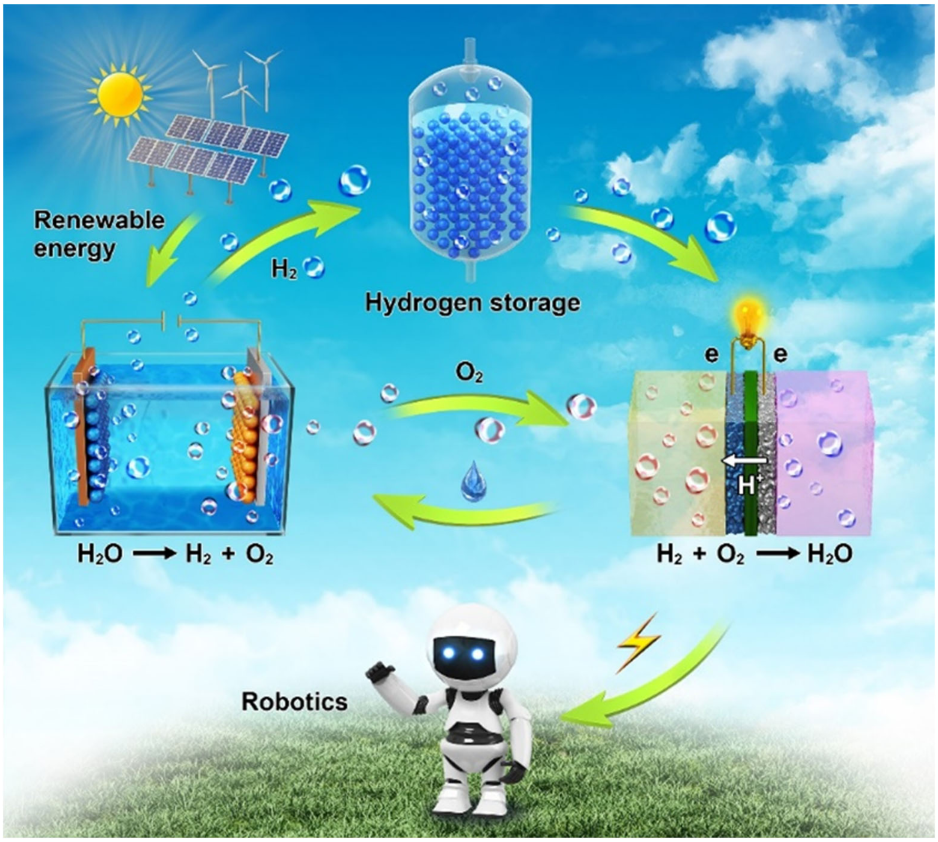

Figure 7. Robots can be powered by the integrated energy system consisting of an electrocatalytic water-splitting unit powered by on-site PSCs to produce O_2 and H_2 gases for a fuel cell to generate clean electricity from sunlight and water.

materials showed a remarkably high gravimetric density of up to 7.6 wt% for H_2 storage at ambient conditions, reusability was only up to two or three cycles.[92] Thus, porous materials, including zeolites, carbon nanomaterials (e.g., carbon nanotubes, graphene), metal–organic frameworks (MOFs), and covalent organic frameworks (COFs), have also been studied for hydrogen storage.[93] None of these materials have satisfied the norms set by the USA Department of Energy for hydrogen storage at ambient temperature, though some promising results at cryogenic temperature (e.g., 14.0 wt% and 46.2 g L^{-1}) have been achieved with certain MOF materials,[94] leading to potential applications. Indeed, a hydrogen fuel cell combined with metal hydride tanks (Tropical S.A. Company, Athens) has been used as the energy source in robotic tractors for precision agriculture, offering a power range from 0.5 to 5 kW at a specific hydrogen consumption of $\approx$0.74 Nm^3 Kwh^{-1}.[95] Therefore, metal hydrides have great potential for safe and reliable hydrogen storage.[96] Hybridization of metal hydrides with porous MOFs or nanocarbon materials could show synergistic effects to enhance further their hydrogen storage performance.

To operate wirelessly in remote environments (e.g., in outer space), robots must extract useful energy from their surroundings for highly energy dense storage and long-term operation (e.g., long-range unmanned aerial vehicles, UAVs). Solar energy, derived directly from readily available sunlight, is a free and renewable power source with zero pollutant emissions, but it is intrinsically intermittent. This limitation can be overcome by integrating solar cell(s) with an energy storage unit(s), such as a battery or supercapacitor,[97] to continuously supplying electricity as a sustainable power source for mobile robots with special missions, as exemplified by some long-range UAVs (e.g., Zephyr Stratospheric UAV and solar-powered next technology robots). On the other hand, certain C-MFECs have been recently demonstrated to be active even toward the CO_2 reduction reaction (CO_2RR) and N_2 reduction reaction (NRR) for chemical energy conversion.[98] Based on the reversible redox reaction with CO_2RR, which forms lithium carbonate and carbon via $4Li^+ + 3CO_2 + 4e^- = C + 2Li_2CO_3$ ($E_0 = 2.8$ V vs Li/Li^+, 1876 Wh kg^{-1})[99] during the discharge process and decomposes Li_2CO_3 upon charging, Li–CO_2 batteries have been developed to capture CO_2 and deliver an energy density up to 1876 Wh kg^{-1}.[100] The CO_2-powered batteries can not only mitigate the emission of CO_2 from fossil fuel combustion but also hold promise as a form of high-density energy to power robots for space exploration missions on Mars where the atmosphere ($\approx$96% CO_2) provides an in situ CO_2 resource that is nearly ideal in composition for the CO_2-powered battery to function.[101]

6.4. Power Schemes for Ultrasmall Machines

The concept of miniaturizing surgical machines into ultrasmall counterparts that can be swallowed for medical treatment was envisioned by Richard Feynman in his seminal lecture in 1959. Until recent decades, we have witnessed the rapid development of ultrasmall motors and machines in molecular-to-micrometer scales. Progress has been made in all aspects, including propulsion mechanisms, fabrication assembly strategies, performance optimization, and applications. However, these significant advances have not resulted in a breakthrough that has allowed us to miniaturize directly complex macroscopic machines. This task remains challenging owing to the small size and sophisticated design of traditional machines. Rather, myriad ultrasmall machines that mirror their macroscopic counterparts have been created by exploring the distinct physics and chemistry at small scales, which dominate interaction and locomotion of all small objects with surroundings. In the following sections, we discuss an array of integrated powering schemes utilized by various ultrasmall motors that exist in nature ubiquitously or are made artificially. The same powering schemes could be adopted to propel future micro-/nanorobots.

6.5. Motor Proteins

Nature has created extremely small machines that were highly efficient before the emergence of human beings on Earth. Motor proteins are molecular motors that convert chemical energy into mechanical energy to accomplish essential biological functions, including transporting cargos and generating mechanical propulsion.[102] They are essential to life and can be found in all organisms.[5,103] Below, we examine the powering mechanisms of two representative molecular motors, that is, the kinesin-1 and the bacteria flagellar that can transport and rotate, respectively (**Figure** 8A,B).

Kinesin-1 motors belong to a family of microtubular protein motors. They are powered by adenosine triphosphate (ATP) hydrolysis to support intracellular transport processes along microtubule cytoskeletons in cells.[103a,104] A kinesin walks forward along the microtubules in a hand-over-hand stepping with a constant step size of 8 nm per ATP hydrolysis (Figure 8A).[105] The stall force is ≈6 pN, the maximum speed with an adequate ATP supply is ≈800 nm s^{-1}, and the efficiency of energy conversion can reach 50%.[103a,106]

Bacteria flagellar motors are types of molecular machines that can reversibly rotate helical filaments to propel the locomotion of bacteria cells.[5] The motors operate by harnessing free energy released from ions transported across cytoplasmic membranes with a downhill electrochemical gradient. They can rotate up to a speed of ≈300 and 1700 rps. when driven by a gradient of hydrogen and sodium ions, respectively.[107] The energy conversion efficiency is estimated to be near unity, that is, ≈90%.[108]

6.6. Artificial Molecular Motors

Over the last few decades, numerous organic molecular motors have been synthetized, either by learning from nature or by mimicking simple macroscopic machines.[109] In 2016, the Nobel Prize in Chemistry was awarded to Jean-Pierre Sauvage, Sir J. Fraser Stoddart, and Bernard L. Feringa for their original contributions to artificial molecular machines. Comprehensive reviews have been given by the main contributors. Here, a few representative works are selected for discussion. Stoddart et al. reported a rotaxane molecular shuttle made of macrocycle

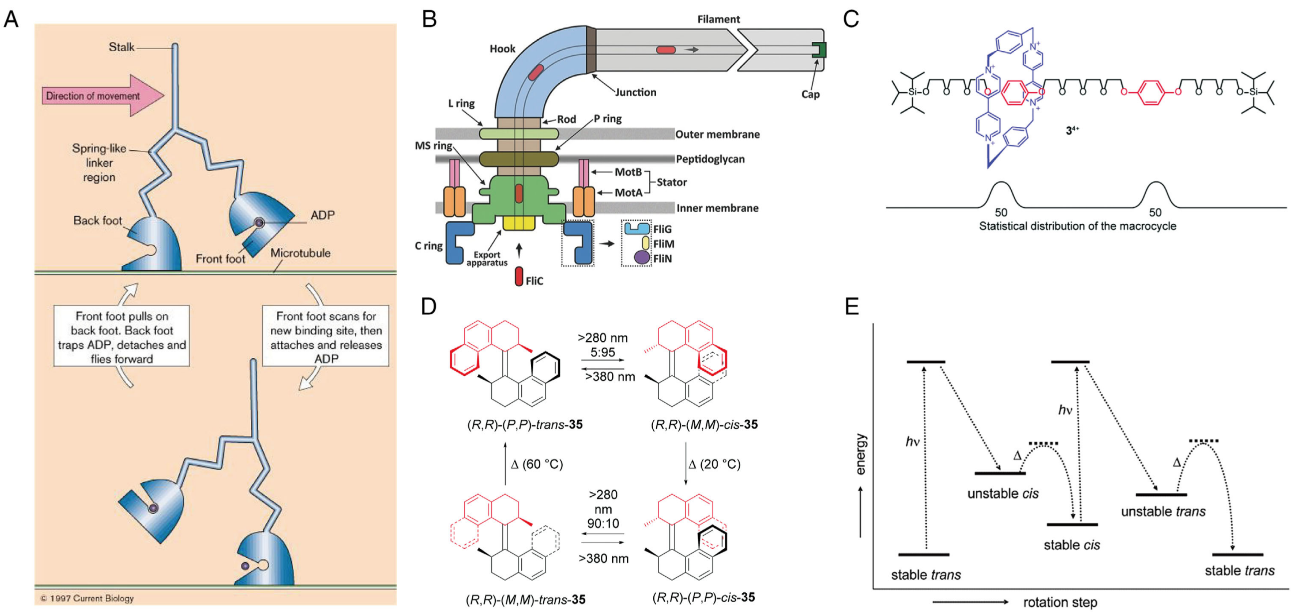

Figure 8. Schematic of molecular motors. A) The walking mechanism of a kinesin molecule. Reproduced with permission.[104b] Copyright 1997, Cell Press. B) The structural components of a bacterial flagellar motor. Reproduced with permission.[107b] Copyright 2015, Wiley. C) The first synthesized molecular shuttle that can transit between two binding sites. D) The structure and working mechanism of the light-driven rotary molecular motor. E) The energy profile during the 360° unidirectional rotation. Reproduced with permission.[109b] Copyright 2015, American Chemical Society.

molecules threaded in an axle molecular track that can operate between two binding sites with equivalent distribution possibilities, as shown in Figure 8C. It is the energy from thermal fluctuation that drives the mechanical transition.[110] Later, the transition can select a preferred binding end with an external stimulus, such as pH.[111] The first rotary synthetic molecular motor was reported by Feringa et al. in 1999; it could carry out cyclic unidirectional rotation by energy from UV irradiation.[112] The motor is made of the overcrowded alkene with two identical groups connected by a carbon–carbon double bond. A 360° rotation can be accomplished by transforming the molecule into four different isomers sequentially (Figure 8D). The energy profile during the rotation is depicted in Figure 8E. This light-fueled rotary motor has a quantum efficiency of ≈2%, limited by the cis–trans–photoisomerization step.[113]

6.7. Biological and Bioinspired Micro-/Nanopropellers

In the range of micro-/nanometers, self-propelling motors/machines also prevail in nature. Biological motors, such as flagella and motile cilia, are essential in locomotion of microorganisms to seek for food and light.[114] The directional propulsion of microorganisms arises from the interaction of the mechanical motion of the biological propellers with their surrounding medium. Two actuation modes are commonly observed, that is, corkscrew rotation and flexible filament beating, as shown in **Figure 9**A.

E. coli bacterial cells with a dimension of several micrometers in length and 0.5 µm in diameter are widely found in natural water. An *E coli* cell's propeller is made of several helical flagellum bundles (usually made of four) attached to flagellar motors that rotate counterclockwise and drive the helical bundle into corkscrew rotation (Figure 9A). The corkscrew rotation interacts intimately with the surrounding suspension due to viscous drag, resulting in the conversion of rotary motion into linear propulsion of the cells. Both experimental and theoretical studies indicate that the efficiency, defined by the ratio between the net energy used for propulsion and the total energy input from the chemical conversion, is around 2%. This relatively low efficiency can be attributed to the dissipation due to the viscous force on both the rotating filament bundles and the cell.[115] The natural corkscrew structures and powering mechanism inspired the creation of several exquisite artificial helical micro-/nanopropellers with defined structures and compositions on a large scale.[116] In a classical example, to mimic the swimming manner of the bacterial flagella, a ferromagnetic segment is integrated as a tiny handle that can rotate a helical structure around its long axis using energy from a uniform rotating magnetic field (Figure 9B). The speed is up to hundreds of rounds per second. Catalytic reactions were also introduced to drive a helical structure that can spin and transport.[117]

Planar beating of flagella is another useful propulsion strategy adopted by spermatozoa and many other Eukaryotes (Figure 9C).[118] The beating of the flexible flagellar generates a nonreciprocal motion that propels the linked head forward. The propulsion mechanism has been systematically studied[119] and further has inspired the design of several innovative artificial motors made of flexible bodies powered by harnessing energy from external magnetic, optical, and acoustic fields (Figure 9D). The propulsion efficiency resides at around 1% or less.[120]

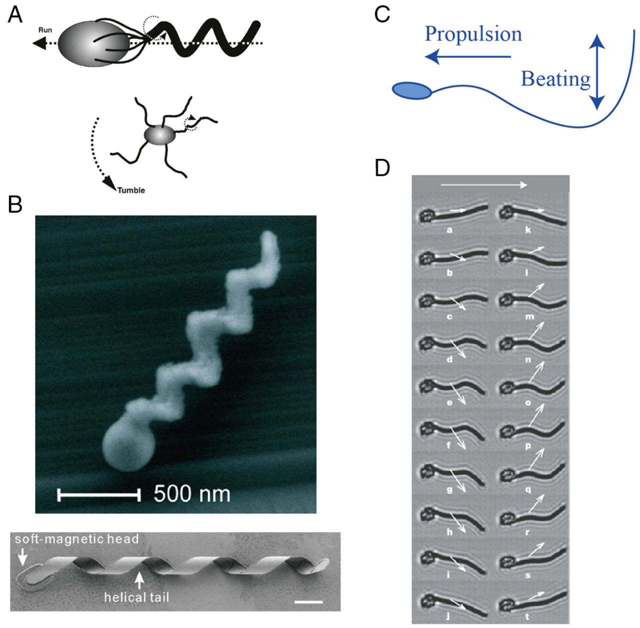

Figure 9. Bioinspired propulsion at low Reynolds numbers. A) The locomotion of *E. coli*. In "Run" mode, the flagella are bundled due to counterclockwise rotation and propel the *E. coli* to swim forward. In "Tumble" mode, flagella rotate clockwise and cause spinning of the cell. Reproduced with permission.[114c] Copyright 2010, AIP Publishing. B) Artificial magnetic helix micro-/nanoswimmers fabricated by two different methods that mimic the propulsion of flagella. Reproduced with permission.[116a] Copyright 2009, American Chemical Society; Reproduced with permission.[116b] Copyright 2009, AIP Publishing. C) Schematic of locomotion of a sperm that beats its flexible tail. D) Agile micromotors driven by a magnetic field that mimics the propulsion of a sperm. Reproduced with permission.[120] Copyright 2005, Springer Nature.

6.8. Powering Micro-/Nanoswimmers by Designing Broken Symmetry

At the micro-/nanoscale, physical principles that govern a moving object differ from those in the macroscopic world. When an ultrasmall object swims in water, the viscous drag overwhelms its inertia, which can be shown by the Reynolds number (R). For a bacteria cell and a similar-sized artificial propeller, the Reynolds number is at around 10^{-4} to 10^{-5}, 8–9 orders of magnitude lower than that of a human swimming in water. It has been shown that in such an extremely-low-Reynolds-number region, no object can make any net movement in a Newtonian medium if exerting a time-symmetric propulsion (scallop theorem).[121] A net propulsion at a low-Reynolds-number region requires broken symmetry. With this understanding, a series of innovative artificial micro-/nanoscale motors have been designed and sculptured by breaking their symmetries in physical fields or chemical reactions or exploiting asymmetrical properties of their suspension medium.[122]

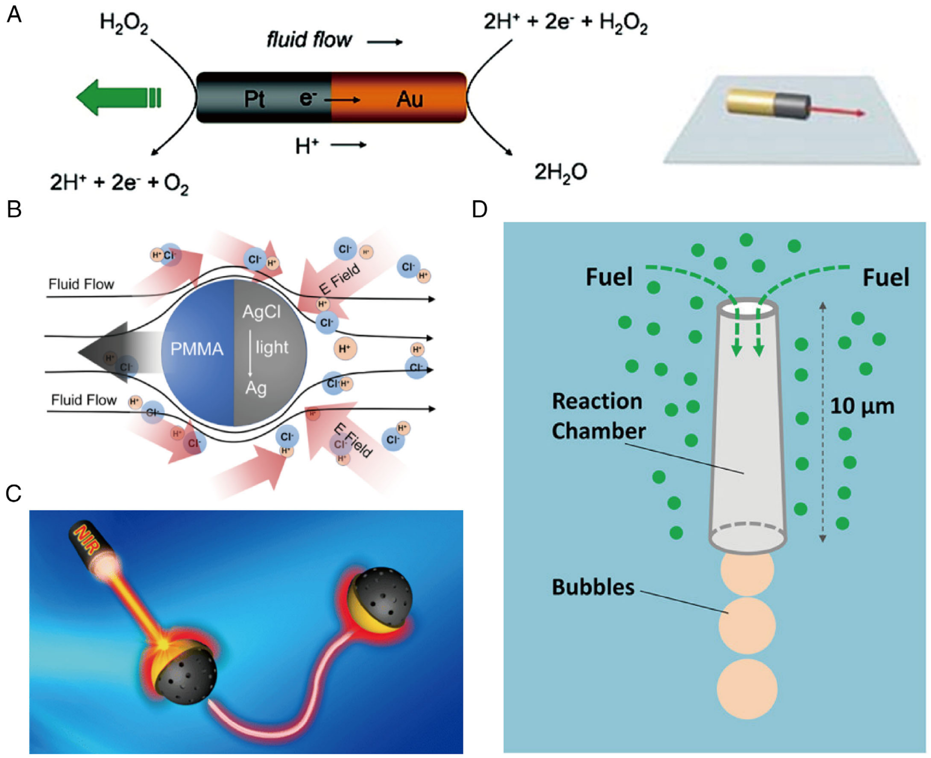

Figure 10. Self-propelling micromotors with designed broken symmetry. A) A bimetallic nanorod motor that consumes H_2O_2 fuel and generates locomotion by self-electrophoresis. Reproduced with permission.[122a] Copyright 2013, Elsevier. B) A UV light-actuated PMMA/AgCl Janus motor generating locomotion by self-diffusiophoresis. Reproduced with permission.[126] Copyright 2018, American Chemical Society. C) A near-infrared laser-actuated silica/Au Janus micromotor propelled by thermophoresis. Reproduced with permission.[128] Copyright 2016, American Chemical Society. D) A tubular micromotor with catalytic coating inside the tube being propelled by bubble formation and detachment. Reproduced with permission.[129a] Copyright 2016, American Chemical Society.

Elegant examples have been demonstrated by breaking the symmetry of ionic distribution in the vicinity of a micro-/nanomotor. A well-known work was reported on a Pt/Au micromotor, which can propel in a hydroperoxide (H_2O_2) solution by the electric field generated from different ions produced on the respective Pt and Au segments in the catalytic reaction (**Figure 10**A). This working mechanism is the so-called self-electrophoresis that has received immense interest owing to its essential role in converting chemical energy into mechanical propulsion in an artificial system.[123] However, the efficiency is usually low, on the order of 10^{-8}–10^{-9}. The majority of the chemical energy is dissipated by heat, side reactions, viscous drag, and liquid flows induced in the reaction.[124]

Artificial micro-/nanomotors also propel by the so-called self-diffusiophoresis due to the directional flows from asymmetric distribution of chemical species, either ionic or neutron.[125] The detailed mechanism can be ascribed to electrophoretic interaction, chemiphoresis pressure,[125c,126] and steric effect (non-electrolyte diffusiophoresis)[127] depending on the charges of the chemical species. The efficiency is around 10^{-9}. Here, to generate the asymmetric chemical reaction, light has been widely used as the driving power to create a one-side reaction or distinct reactions on Janus semiconductor micro-/nanomotors in aqueous suspension (Figure 10B).[125c]

Micro-/nanoscale motors also self-propel via generating non-uniform local heat distribution, namely, self-thermophoresis. A simple motor of this kind can be made of a silica microsphere with half-coated gold, as shown in Figure 1C.[128] Upon illumination by a 1064 nm laser, the gold coating effectively adsorbs the light and generates a much greater amount of heat than that of the Si hemisphere, which leads to a localized temperature gradient. The motor is thus propelled with speed proportional to the temperature gradient (∇T) and thermodiffusion coefficient (D_T), given by $v = -D_T \nabla T$. The energy efficiency of $10^{-13}$is among the lowest.

Direct bubble propulsion is another power source that requires a rapid chemical reaction to generate gas-phase products distributing asymmetrically near a motor.[129] A representative bubble motor is made of a conical tube (Figure 10D) that consists of a catalytic layer of Pt at the inner surface that decomposes H_2O_2 fuel into oxygen molecules. When the oxygen molecules enrich into a bubble of a threshold size, it departs from the motor with a strong and instant thrust that propels the motor.[130] The energy efficiency is estimated to be around 10^{-9}. In addition, several notable mechanisms have been demonstrated to introduce asymmetry to a micro-/nanomotor, including propelling near a solid wall,[131] generating asymmetric body deformation with dynamic light patterning,[132] and actuation in non-

Newtonian liquid.[133] The energy sources include optical and magnetic fields.

6.9. Powering by Energy from an External Tweezing Field

Unlike the self-propelled motors that generate local thrusts for actuation, another class of motors is propelled via directly interacting and transferring propulsion momentum from an external physical field. These manipulations are more commonly termed as tweezing techniques, including optical,[134] electric,[135] magnetic,[136] and acoustic tweezers.[137]

Optical tweezers are powerful tools in manipulating objects around or below several micrometers. They utilize a highly focused laser beam to generate an optical trap (or barrier) for manipulating micro-/nanoparticles near the focal plane by optical gradient forces (**Figure 11**A).[134] Holographic beams allow not only trapping, but also the individual or simultaneous movement of multiple particles via independent manipulation of optical traps.[138] The electric manipulations are able to exert a net force and an alignment torque upon a particle by applying a combined AC and DC electric field (Figure 11B). The force is generated by electrophoresis/electroosmosis for a charged particle; the torque is created by the interaction between the AC field and the polarized particle. Optoelectric tweezers utilize dielectrophoretic (DEP) forces from a localized field gradient patterned by light on an electrically powered light-sensitive substrate (Figure 11C).[139] Furthermore, rotational torques can be generated from an electric field, that is, electrorotation and electroorientation in a high-frequency AC electric field.[140] Acoustic manipulations leverage the acoustic radiation force induced by either standing waves or traveling waves to manipulate particles.[137] Standing-wave acoustic tweezers generate ordered arrays of pressure nodes in the field where many particles can be trapped into ordered arrays.[141] Traveling-wave acoustic tweezers, that is, acoustic hologram, can create pressure nodes with arbitrary 3D patterns by modulating the phase of the wave actively or passively (Figure 11D).[142] Magnetic tweezers exert forces to magnetic micro-/nanoobjects in the direction of the local magnetic field gradient and apply alignment torques in the direction of the local magnetic field. (Figure 11E).[136]

To accommodate manipulations with high versatility and/or in complex suspension medium, hybrid powers have recently been exploited, including light-modulated multimode reconfigurable micromotors in electric fields,[143] sperm-powered biohybrid motors steered by magnetic fields,[144] and dual chemical/light-powered motors and chemical/electric field-powered motors with tunable speeds.[145] Research in hybrid-powering mechanisms has enabled the control of different components within a nanorobot for sophisticated operations and the manipulation of individual nanorobots in a swarm for collaborative action.

Myriad demonstrations have shown the great potential of ultrasmall motors in cargo transport, single-cell drug delivery, biochemical sensing, cellular and tissue surgery, and environmental remediation.[11,146] For the readers' interest, we highlight here several groundbreaking applications of ultrasmall artificial robotic motors, including molecular cargo transport by kinesin-driven shuttles,[147] cytokine delivery to single living cells,[148] remote capture of a living tissue sample by magnetic manipulation and thermal triggering,[149] targeted delivery with

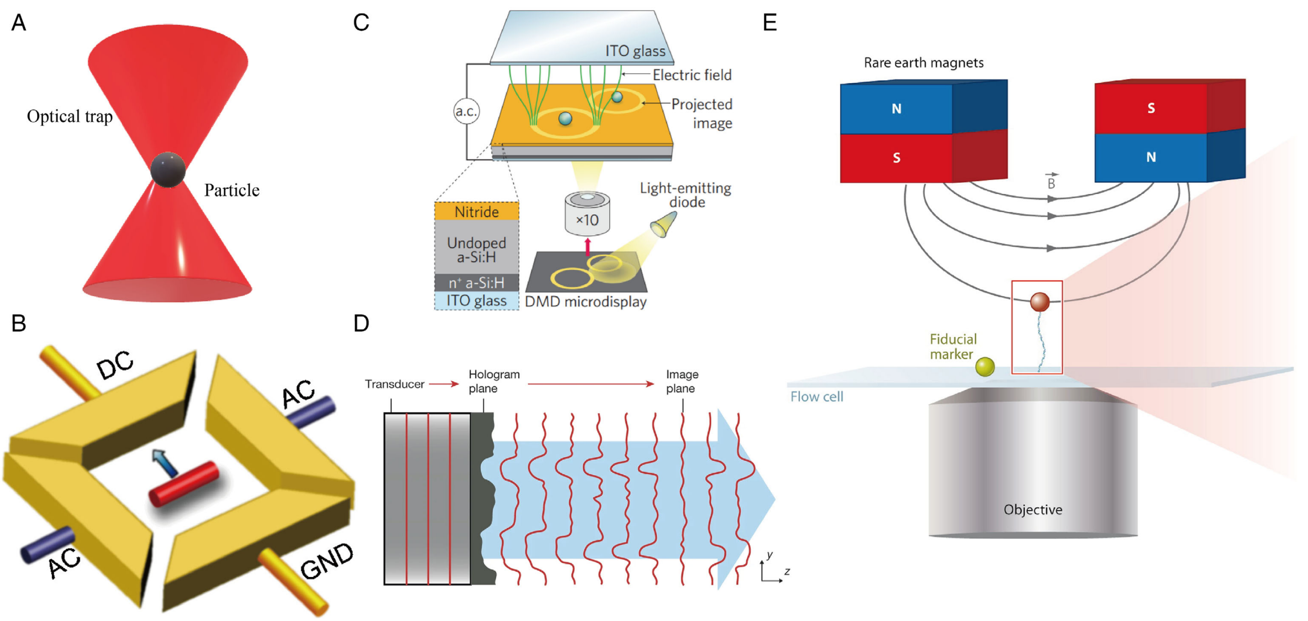

Figure 11. Micro/nanomanipulation/tweezing techniques with externally applied physical fields. A) The optical tweezers trap a microparticle with a laser beam. B) Electric manipulation of longitudinal particles by the combination of AC and DC electrical fields that control orientation and propulsion directions independently. Reproduced with permission.[135] Copyright 2008, AIP Publishing. C) Optoelectronic tweezers trap cells with AC electric fields patterned by light on a photoconductive substrate. Reproduced with permission.[139] Copyright 2005, Springer Nature. D) Holographic acoustic tweezers create arbitrary pressure profiles that can pattern and manipulate particles into prescribed patterns. Reproduced with permission.[142b] Copyright 2016, Springer Nature. E) Magnetic tweezers for the manipulation of magnetic particles. Reproduced with permission.[136] Copyright 2012, Annual Reviews.

nanopropellers in eyes,[150] magnetic microrobot-assisted stem cell transplantation[151] and fertilization[152], and cargo delivery with microrollers against blood flow.[153]

6.10. Prospective

Great progress has been made in energy harvesting and energy storage technologies for self-powered untethered robotics in the past decades. For robots that require relatively low power input, integrating renewable energy harvesting devices could readily offer sufficient power for operation. Different energy harvesting devices have their advantages and limitations. For example, OSCs generally have a relatively high efficiency and high energy density, but their flexibility is limited, and the solar energy varies significantly with time and location; the TENG can be readily flexible or stretchable, but efforts are still required to improve its energy density and energy utilization efficiency. Therefore, it is important to select proper energy technologies as power sources for robots according to their specific applications. Hybrid energy devices/systems are often required to achieve self-powered robots. Thus, future research on power management circuits for robots is also required to deal with hybrid systems and maximize the energy utilization efficiency.

For a high-power robot, a precharged or fueled energy storage device is one of the most viable options. With continued advances in robotics, the demands for power systems have become more rigorous, particularly in pursuing higher power and energy density with safer operation and longer cycle life. The constraints for powering untethered robotics are far more challenging since their operation environments, structures and shapes, and performance metrics are usually different and more complex compared with the existing portable electronic devices and electric vehicles.

For micro-/nanoscale artificial robots, we note that a powering mechanism with an extremely low efficiency still allows for various tasks to be accomplished owing to the much-reduced energy demand at a low dimension. Therefore, self-powered microrobots have less concerns in terms of energy consumption or efficiency, but they are more restricted by their distinct working principles, structural designs, material selections, and application limitations. This is in stark contrast to natural existing biological motors that exhibit an energy efficiency up to almost a unity. In living beings without such a high energy efficiency, however, the required energy intake can be extraordinary for various molecular motors to enable large-scale locomotion. Therefore, it is highly desirable to significantly improve the energy conversion efficiency for the counterpart artificial microrobots to make a prominent impact at a macroscopic scale. This improvement requires further advancements in renewable energy technologies and associated materials that are scalable to small scale.[154] In the past several decades, the field of electrochemical energy storage has seen challenges in innovating a single battery chemistry or supercapacitor device that can deliver desired multifunctional performances, including high power, high energy density, safe operation, and a long cycle life. The constraints posed by various AMRs add other difficulties. To alleviate these issues, one may consider implementing an integrated energy system consisting of several technologies based on batteries, supercapacitors, fuel cells, solar panels, and actuators with control and thermal management units, although this strategy may increase the complexity and weight with additional cost.

In parallel, innovative fusion of state-of-the-art energy storage materials with desired functional structures and properties (e.g., capability to withstand elastic and plastic deformations to accommodate for biomorphic shapes) can substantially benefit the future advancement in AMRs. Advanced fabrication techniques, such as multimaterial-embedded 3D printing, micromolding, and lithography, could become key enablers in rapid prototyping and manufacturing of specialized energy storage components (e.g., miniaturized solid oxide fuel cells: micro-SOFCs) to meet the demands for an array of AMRs on different scales. With so many advanced materials, fabrication tools, and renewable energy technologies already reported and more to be developed, there will be vast opportunities for developing numerous innovative single or hybrid power sources for various robots with sophisticated demands for diverse applications. Continued research and development efforts in this exciting field will surely revolutionize the way in which future robots are powered.

Acknowledgements

The work was supported by National Science Foundation (1710922 and 1930649), Welch Foundation F-1734 to DF, and Welch Foundation grant F-1254 to AM.

Conflict of Interest

The authors declare no conflict of interest.

Keywords

all scale, energy harvesting, energy storage, robot

Received: February 15, 2022
Revised: April 5, 2022
Published online:

[1] I. Asimov, in *Understanding Physics*, Vol. *1*, Barnes and Noble Publishing, New York, NY **1988**.
[2] J. Marchant, *Nat. News* **2010**, *468*, 496.
[3] S. A. Ajwad, J. Iqbal, presented at *Int. Conf. on Engineering and Emerging Technologies*, **2015**.
[4] a) R. A. Beasley, *J. Robot.* **2012**, 2012; b) S. K. Srivastava, G. Clergeaud, T. L. Andresen, A. Boisen, *Adv. Drug Deliv. Rev.* **2019**, *138*, 41.
[5] H. C. Berg, *Annu. Rev. Biochem.* **2003**, *72*, 19.
[6] M. A. Green, E. D. Dunlop, J. Hohl-Ebinger, M. Yoshita, N. Kopidakis, A. W. Ho-Baillie, *Progr. Photovolt. Res. Appl.* **2020**, *28*, 3.
[7] C. Wu, A. C. Wang, W. Ding, H. Guo, Z. L. Wang, *Adv. Mater.* **2019**, *9*, 1802906.
[8] S. M. Pourkiaei, M. H. Ahmadi, M. Sadeghzadeh, S. Moosavi, F. Pourfayaz, L. Chen, M. A. P. Yazdi, R. Kumar, *Energy* **2019**, *186*, 115849.
[9] H. Liu, J. Ma, L. Tong, G. Ma, Z. Zheng, M. Yao, *Energies* **2018**, *11*, 513.
[10] Z. Zhang, H. Pang, A. Georgiadis, C. Cecati, *IEEE Trans. Ind. Electron.* **2018**, *66*, 1044.
[11] K. Kim, J. Guo, Z. Liang, D. Fan, *Adv. Funct. Mater.* **2018**, *28*, 1705867.

[12] G.-Z. Yang, J. Bellingham, P. E. Dupont, P. Fischer, L. Floridi, R. Full, N. Jacobstein, V. Kumar, M. McNutt, R. Merrifield, *Sci. Robot.* **2018**, *3*, eaar7650.
[13] M. Luqman, S. R. Ahmad, S. Khan, U. Ahmad, A. Raza, F. Akmal, *Smart Grid Renew. Energy* **2015**, *6*, 128.
[14] S. A. Hashemi, S. Ramakrishna, A. G. Aberle, *Energy Environ. Sci.* **2020**, *13*, 685.
[15] L. Fagiolari, F. Bella, *Energy Environ. Sci.* **2019**, *12*, 3437.
[16] J. Feng, X. Zhu, Z. Yang, X. Zhang, J. Niu, Z. Wang, S. Zuo, S. Priya, S. Liu, D. Yang, *Adv. Mater.* **2018**, *30*, 1801418.
[17] K.-S. Chen, J.-F. Salinas, H.-L. Yip, L. Huo, J. Hou, A. K.-Y. Jen, *Energy Environ. Sci.* **2012**, *5*, 9551.
[18] Z. Xu, T. Li, Q. Liu, F. Zhang, X. Hong, S. Xie, C. Lin, X. Liu, W. Guo, *Sol. Energy Mater. Sol. Cells* **2018**, *179*, 297.
[19] a) M. Peng, X. Yu, X. Cai, Q. Yang, H. Hu, K. Yan, H. Wang, B. Dong, F. Zhu, D. Zou, *Nano Energy* **2014**, *10*, 117; b) T. Chen, L. Qiu, Z. Yang, Z. Cai, J. Ren, H. Li, H. Lin, X. Sun, H. Peng, *Angew. Chem. Int. Ed.* **2012**, *51*, 11977; c) J. Chen, Y. Huang, N. Zhang, H. Zou, R. Liu, C. Tao, X. Fan, Z. L. Wang, *Nat. Energy* **2016**, *1*, 1.
[20] N. Zhang, J. Chen, Y. Huang, W. Guo, J. Yang, J. Du, X. Fan, C. Tao, *Adv. Mater.* **2016**, *28*, 263.
[21] D. H. Shin, S. W. Seo, J. M. Kim, H. S. Lee, S.-H. Choi, *J. Alloys Compd.* **2018**, *744*, 1.
[22] Z. Zhang, X. Li, G. Guan, S. Pan, Z. Zhu, D. Ren, H. Peng, *Angew. Chem., Int. Ed.* **2014**, *53*, 11571.
[23] M. Kaltenbrunner, M. S. White, E. D. Głowacki, T. Sekitani, T. Someya, N. S. Sariciftci, S. Bauer, *Nat. Commun.* **2012**, *3*, 1.
[24] H. Jinno, K. Fukuda, X. Xu, S. Park, Y. Suzuki, M. Koizumi, T. Yokota, I. Osaka, K. Takimiya, T. Someya, *Nat. Energy* **2017**, *2*, 780.
[25] a) T. N. Murakami, N. Kawashima, T. Miyasaka, *Chem. Commun.* **2005**, 3346; b) C. Y. Hsu, H. W. Chen, K. M. Lee, C. W. Hu, K. C. Ho, *J. Power Sources* **2010**, *195*, 6232.
[26] a) C. Li, S. Cong, Z. Tian, Y. Song, L. Yu, C. Lu, Y. Shao, J. Li, G. Zou, M. H. Rümmeli, *Nano Energy* **2019**, *60*, 247; b) Z. Chai, N. Zhang, P. Sun, Y. Huang, C. Zhao, H. J. Fan, X. Fan, W. Mai, *ACS Nano* **2016**, *10*, 9201.
[27] Z. Wen, M.-H. Yeh, H. Guo, J. Wang, Y. Zi, W. Xu, J. Deng, L. Zhu, X. Wang, C. Hu, *Sci. Adv.* **2016**, *2*, 1600097.
[28] X. Xue, S. Wang, W. Guo, Y. Zhang, Z. L. Wang, *Nano Lett.* **2012**, *12*, 5048.
[29] a) J. Cannarella, C. B. Arnold, *Adv. Mater.* **2015**, *27*, 7440; b) Y. Zi, H. Guo, Z. Wen, M.-H. Yeh, C. Hu, Z. L. Wang, *ACS Nano* **2016**, *10*, 4797.
[30] Z. L. Wang, J. Song, *Science* **2006**, *312*, 242.
[31] C. Zhang, W. Fan, S. Wang, Q. Wang, Y. Zhang, K. Dong, *ACS Appl. Electron. Mater.* **2021**, *3*, 2449.
[32] a) X. Pu, M. Liu, X. Chen, J. Sun, C. Du, Y. Zhang, J. Zhai, W. Hu, Z. L. Wang, *Sci. Adv.* **2017**, *3*, 1700015; b) J. Sun, X. Pu, M. Liu, A. Yu, C. Du, J. Zhai, W. Hu, Z. L. Wang, *ACS Nano* **2018**, *12*, 6147.
[33] J. Nie, X. Chen, Z. L. Wang, *Adv. Funct. Mater.* **2019**, *29*, 1806351.
[34] Z. L. Wang, *Nano Energy* **2020**, *68*, 104272.
[35] a) X. Pu, L. Li, M. Liu, C. Jiang, C. Du, Z. Zhao, W. Hu, Z. L. Wang, *Adv. Mater.* **2016**, *28*, 98; b) X. Pu, W. Hu, Z. L. Wang, *Small* **2018**, *14*, 1702817; c) X. Pu, Z. L. Wang, *Chem. Sci.* **2021**, *12*, 34; d) M. Liu, Z. Cong, X. Pu, W. Guo, T. Liu, M. Li, Y. Zhang, W. Hu, Z. L. Wang, *Adv. Funct. Mater.* **2019**, *29*, 1806298; e) S. Wang, Z.-H. Lin, S. Niu, L. Lin, Y. Xie, K. C. Pradel, Z. L. Wang, *ACS Nano* **2013**, *7*, 11263.
[36] a) H. Ouyang, Z. Liu, N. Li, B. Shi, Y. Zou, F. Xie, Y. Ma, Z. Li, H. Li, Q. Zheng, *Nat. Commun.* **2019**, *10*, 1; b) W. Jiang, H. Li, Z. Liu, Z. Li, J. Tian, B. Shi, Y. Zou, H. Ouyang, C. Zhao, L. Zhao, *Adv. Mater.* **2018**, *30*, 1801895; c) Q. Zheng, Y. Zou, Y. Zhang, Z. Liu, B. Shi, X. Wang, Y. Jin, H. Ouyang, Z. Li, Z. L. Wang, *Sci. Adv.* **2016**, *2*, e1501478.
[37] X. Chen, X. Pu, T. Jiang, A. Yu, L. Xu, Z. L. Wang, *Adv. Funct. Mater.* **2017**, *27*, 1603788.
[38] a) C. Zhang, W. Tang, Y. Pang, C. Han, Z. L. Wang, *Adv. Mater.* **2015**, *27*, 719; b) H. Yang, Y. Pang, T. Bu, W. Liu, J. Luo, D. Jiang, C. Zhang, Z. L. Wang, *Nat. Commun.* **2019**, *10*, 1.
[39] a) Y. Wang, X. Y. Wei, S. Y. Kuang, H. Y. Li, Y. H. Chen, F. Liang, L. Su, Z. L. Wang, G. Zhu, *ACS Nano* **2018**, *12*, 441; b) L. Zheng, Y. Wu, X. Chen, A. Yu, L. Xu, Y. Liu, H. Li, Z. L. Wang, *Adv. Funct. Mater.* **2017**, *27*, 1606408; c) J. Nie, Z. Ren, J. Shao, C. Deng, L. Xu, X. Chen, M. Li, Z. L. Wang, *ACS Nano* **2018**, *12*, 1491; d) J. Cheng, W. Ding, Y. Zi, Y. Lu, L. Ji, F. Liu, C. Wu, Z. L. Wang, *Nat. Commun.* **2018**, *9*, 1.
[40] Q. Hua, J. Sun, H. Liu, R. Bao, R. Yu, J. Zhai, C. Pan, Z. L. Wang, *Nat. Commun.* **2018**, *9*, 1.
[41] M. Zhu, Z. Sun, Z. Zhang, Q. Shi, T. He, H. Liu, T. Chen, C. Lee, *Sci. Adv.* **2020**, *6*, eaaz8693.
[42] H. Guo, X. Pu, J. Chen, Y. Meng, M.-H. Yeh, G. Liu, Q. Tang, B. Chen, D. Liu, S. Qi, *Sci. Robot.* **2018**, *3*.
[43] Z. Wang, J. An, J. Nie, J. Luo, J. Shao, T. Jiang, B. Chen, W. Tang, Z. L. Wang, *Adv. Mater.* **2020**, *32*, 2001466.
[44] Y. C. Lai, J. Deng, R. Liu, Y. C. Hsiao, S. L. Zhang, W. Peng, H. M. Wu, X. Wang, Z. L. Wang, *Adv. Mater.* **2018**, *30*, 1801114.
[45] X. Pu, H. Guo, J. Chen, X. Wang, Y. Xi, C. Hu, Z. L. Wang, *Sci. Adv.* **2017**, *3*, 1700694.
[46] a) Z. Zhang, T. He, M. Zhu, Z. Sun, Q. Shi, J. Zhu, B. Dong, M. R. Yuce, C. Lee, *NPJ Flex. Electron.* **2020**, *4*, 1; b) T. Jin, Z. Sun, L. Li, Q. Zhang, M. Zhu, Z. Zhang, G. Yuan, T. Chen, Y. Tian, X. Hou, *Nat. Commun.* **2020**, *11*, 1.
[47] a) S. S. Rana, M. A. Zahed, M. T. Rahman, M. Salauddin, S. H. Lee, C. Park, P. Maharjan, T. Bhatta, K. Shrestha, J. Y. Park, *Adv. Funct. Mater.* **2021**, *31*, 2105110; b) Y. Lin, S. Duan, D. Zhu, Y. Li, B. Wang, J. Wu, *Adv. Intell. Syst.* **2021**, *2* 100120.
[48] J. Chen, K. Han, J. Luo, L. Xu, W. Tang, Z. L. Wang, *Nano Energy* **2020**, *77*, 105171.
[49] W. Liu, Z. Wang, G. Wang, G. Liu, J. Chen, X. Pu, Y. Xi, X. Wang, H. Guo, C. Hu, *Nat. Commun.* **2019**, *10*, 1.
[50] W. Liu, Z. Wang, G. Wang, Q. Zeng, W. He, L. Liu, X. Wang, Y. Xi, H. Guo, C. Hu, *Nat. Commun.* **2020**, *11*, 1.
[51] S. J. Kim, J. H. We, B. J. Cho, *Energy Environ. Sci.* **2014**, *7*, 1959.
[52] J. Y. Oh, J. H. Lee, S. W. Han, S. S. Chae, E. J. Bae, Y. H. Kang, W. J. Choi, S. Y. Cho, J.-O. Lee, H. K. Baik, *Energy Environ. Sci.* **2016**, *9*, 1696.
[53] Y. Chen, Y. Zhao, Z. Liang, *Energy Environ. Sci.* **2015**, *8*, 401.
[54] a) Y. Wang, L. Yang, X. L. Shi, X. Shi, L. Chen, M. S. Dargusch, J. Zou, Z. G. Chen, *Adv. Mater.* **2019**, *31*, 1807 916; b) A. Nozariasbmarz, H. Collins, K. Dsouza, M. H. Polash, M. Hosseini, M. Hyland, J. Liu, A. Malhotra, F. M. Ortiz, F. Mohaddes, *Appl. Energy* **2020**, *258*, 114069.
[55] a) C. S. Kim, H. M. Yang, J. Lee, G. S. Lee, H. Choi, Y. J. Kim, S. H. Lim, S. H. Cho, B. J. Cho, *ACS Energy Lett.* **2018**, *3*, 501; b) F. Suarez, A. Nozariasbmarz, D. Vashaee, M. C. Öztürk, *Energy Environ. Sci.* **2016**, *9*, 2099.
[56] Y. Wang, W. Zhu, Y. Deng, B. Fu, P. Zhu, Y. Yu, J. Li, J. Guo, *Nano Energy* **2020**, *73*, 104773.
[57] Y. J. Kim, H. M. Gu, C. S. Kim, H. Choi, G. Lee, S. Kim, K. Y. Kevin, S. G. Lee, B. J. Cho, *Energy* **2018**, *162*, 526.
[58] K. Xu, *Chem. Rev.* **2004**, *104*, 4303.
[59] J. He, A. Manthiram, *Adv. Mater.* **2020**, *10*, 1903241.
[60] A. Manthiram, *Nat. Commun.* **2020**, *11*, 1.
[61] a) K. Song, D. A. Agyeman, M. Park, J. Yang, Y. M. Kang, *Adv. Mater.* **2017**, *29*, 1606572; b) J. He, L. Luo, Y. Chen, A. Manthiram, *Adv.*

Mater. **2017**, *29*, 1702707; c) Y. You, H. R. Yao, S. Xin, Y. X. Yin, T. T. Zuo, C. P. Yang, Y. G. Guo, Y. Cui, L. J. Wan, J. B. Goodenough, *Adv. Mater.* **2016**, *28*, 7243.
[62] C. Zhang, L. Zhang, Y. Ding, S. Peng, X. Guo, Y. Zhao, G. He, G. Yu, *Energy Storage Mater.* **2018**, *15*, 324.
[63] C. A. Aubin, S. Choudhury, R. Jerch, L. A. Archer, J. H. Pikul, R. F. Shepherd, *Nature* **2019**, *571*, 51.
[64] a) D. Wirthl, R. Pichler, M. Drack, G. Kettlguber, R. Moser, R. Gerstmayr, F. Hartmann, E. Bradt, R. Kaltseis, C. M. Siket, *Sci. Adv.* **2017**, *3*, 1700053; b) A. M. Zamarayeva, A. E. Ostfeld, M. Wang, J. K. Duey, I. Deckman, B. P. Lechêne, G. Davies, D. A. Steingart, A. C. Arias, *Sci. Adv.* **2017**, *3*, 1602051; c) W. J. Song, S. Yoo, G. Song, S. Lee, M. Kong, J. Rim, U. Jeong, S. Park, *Batteries Supercaps* **2019**, *2*, 181.
[65] M. Wang, D. Vecchio, C. Wang, A. Emre, X. Xiao, Z. Jiang, P. Bogdan, Y. Huang, N. A. Kotov, *Sci. Robot.* **2020**, 5.
[66] H. D. Yoo, E. Markevich, G. Salitra, D. Sharon, D. Aurbach, *Mater. Today* **2014**, *17*, 110.
[67] a) H. Park, J. W. Kim, S. Y. Hong, G. Lee, H. Lee, C. Song, K. Keum, Y. R. Jeong, S. W. Jin, D. S. Kim, *ACS Nano* **2019**, *13*, 10469; b) T. An, W. Cheng, *J. Mater. Chem. A* **2018**, *6*, 15478.
[68] a) W. Lu, J.-B. Baek, L. Dai, in *Carbon Nanomaterials for Advanced Energy Systems: Advances in Materials Synthesis and Device Applications*, John Wiley & Sons, Hoboken, NJ **2015**; b) J. R. Miller, P. Simon, *Sci. Mag.* **2008**, *321*, 651.
[69] a) J. B. Goodenough, *Nat. Electron.* **2018**, *1*, 204; b) W. Li, B. Song, A. Manthiram, *Chem. Soc. Rev.* **2017**, *46*, 3006.
[70] M. Winter, R. J. Brodd, *Chem. Rev.* **2004**, *104*, 4245.
[71] C. Hu, Y. Xiao, Y. Zou, L. Dai, *Electrochem. Energy Rev.* **2018**, *1*, 84.
[72] C. Liu, F. Li, L. P. Ma, H. M. Cheng, *Adv. Mater.* **2010**, *22*, E28.
[73] a) S. Sabihuddin, A. E. Kiprakis, M. Mueller, *Energies* **2015**, *8*, 172; b) Y. Liang, C. Z. Zhao, H. Yuan, Y. Chen, W. Zhang, J. Q. Huang, D. Yu, Y. Liu, M. M. Titirici, Y. L. Chueh, *InfoMat* **2019**, *1*, 6.
[74] V. Gurau, T. Armstrong-Koch, *Energies* **2015**, *8*, 9452.
[75] V. Hacker, S. Mitsushima, in *Fuel Cells and Hydrogen: from Fundamentals to Applied Research*, Elsevier, Amsterdam **2018**.
[76] I. E. L. Stephens, J. Rossmeisl, I. Chorkendorff, *Science* **2016**, *354*, 1378.
[77] A. B. Desbiens, J.-P. L. Bigué, C. Véronneau, P. Masson, K. Iagnemma, J.-S. Plante, *Soft Robot.* **2017**, *4*, 367.
[78] A. Wilhelm, B. Surgenor, J. Pharoah, presented at *IEEE Int. Conf. Mechatronics and Automation*, IEEE, Piscataway, NJ **2005**.
[79] S. Chu, Y. Cui, N. Liu, *Nat. Mater.* **2017**, *16*, 16.
[80] A. Sulaiman, F. Inambao, G. Bright, *IOP Conf. Series: Mater. Sci. Eng.* **2014**, *65*, 012003.
[81] a) D. Dunn-Rankin, E. M. Leal, D. C. Walther, *Prog. Energy Combust. Sci.* **2005**, *31*, 422; b) C. Majidi, *Soft Robot.* **2014**, *1*, 5; c) H. T. Hwang, A. Varma, *Curr. Opin. Chem. Eng.* **2014**, *5*, 42.
[82] I. Dincer, M. A. Rosen, *Energy Sustain. Dev.* **2011**, *15*, 137.
[83] C. Hu, L. Dai, *Angew. Chem. Int. Ed.* **2016**, *55*, 11736.
[84] C. Hu, X. Chen, Q. Dai, M. Wang, L. Qu, L. Dai, *Nano Energy* **2017**, *41*, 367.
[85] a) A. Ali, P. K. Shen, *Carbon Energy* **2020**, *2*, 99; b) Z. Zhuang, S. A. Giles, J. Zheng, G. R. Jenness, S. Caratzoulas, D. G. Vlachos, Y. Yan, *Nat. Commun.* **2016**, *7*, 1.
[86] a) K. Gong, F. Du, Z. Xia, M. Durstock, L. Dai, *Science* **2009**, *323*, 760; b) X. Liu, L. Dai, *Nat. Rev. Mater.* **2016**, *1*, 1; c) R. Paul, Q. Dai, C. Hu, L. Dai, *Carbon Energy* **2019**, *1*, 19.
[87] J. Shui, M. Wang, F. Du, L. Dai, *Sci. Adv.* **2015**, *1*, e1400129.
[88] J. Zhang, Z. Zhao, Z. Xia, L. Dai, *Nat. Nanotechnol.* **2015**, *10*, 444.
[89] J. Zhang, L. Dai, *Angew. Chem. Int. Ed.* **2016**, *55*, 13296.
[90] a) Ø. Ulleberg, S. Mørner, *Sol. Energy* **1997**, *59*, 271; b) T. Yoshida, K. Kojima, *Electrochem. Soc. Interfaces* **2015**, *24*, 45.
[91] a) D. P. Broom, in *Hydrogen Storage Materials: The Characterisation of their Storage Properties*, Springer Science & Business Media, Cham **2011**; b) K. Hirose, in *Handbook of Hydrogen Storage: New Materials for Future Energy Storage*, John Wiley & Sons, Hoboken, NJ **2010**.
[92] B. Sakintuna, F. Lamari-Darkrim, M. Hirscher, *Int. J. Hydrogen Energy* **2007**, *32*, 1121.
[93] a) V. Verdinelli, A. Juan, E. German, *Int. J. Hydrogen Energy* **2019**, *44*, 8376; b) Y. Guo, X. Lan, J. Cao, B. Xu, Y. Xia, J. Yin, Z. Liu, *Int. J. Hydrogen Energy* **2013**, *38*, 3987; c) S. L. James, *Chem. Soc. Rev.* **2003**, *32*, 276; d) R. E. Morris, P. S. Wheatley, *Angew. Chem. Int. Ed.* **2008**, *47*, 4966; e) V. Jain, B. Kandasubramanian, *J. Mater. Sci.* **2020**, *55*, 1865; f) J. L. Rowsell, O. M. Yaghi, *Angew. Chem. Int. Ed.* **2005**, *44*, 4670.
[94] Z. Chen, P. Li, R. Anderson, X. Wang, X. Zhang, L. Robison, L. R. Redfern, S. Moribe, T. Islamoglu, D. A. Gómez-Gualdrón, *Science* **2020**, *368*, 297.
[95] M. Gonzalez-de-Soto, L. Emmi, C. Benavides, I. Garcia, P. Gonzalez-de-Santos, *Biosys. Eng.* **2016**, *143*, 79.
[96] S. Jeong, T. W. Heo, J. Oktawiec, R. Shi, S. Kang, J. L. White, A. Schneemann, E. W. Zaia, L. F. Wan, K. G. Ray, *ACS Nano* **2020**, *14*, 1745.
[97] a) J. Xu, Y. Chen, L. Dai, *Nat. Commun.* **2015**, *6*, 1; b) P. Thounthong, V. Chunkag, P. Sethakul, S. Sikkabut, S. Pierfederici, B. Davat, *J. Power Sources* **2011**, *196*, 313; c) X. Xu, S. Li, H. Zhang, Y. Shen, S. M. Zakeeruddin, M. Graetzel, Y.-B. Cheng, M. Wang, *ACS Nano* **2015**, *9*, 1782.
[98] L. Dai, *Adv. Mater.* **2019**, *31*, 1900973.
[99] Y. Qiao, J. Yi, S. Wu, Y. Liu, S. Yang, P. He, H. Zhou, *Joule* **2017**, *1*, 359.
[100] a) L. Song, C. Hu, Y. Xiao, J. He, Y. Lin, J. W. Connell, L. Dai, *Nano Energy* **2020**, *71*, 104595; b) C. Hu, L. Gong, Y. Xiao, Y. Yuan, N. M. Bedford, Z. Xia, L. Ma, T. Wu, Y. Lin, J. W. Connell, *Adv. Mater.* **2020**, *32*, 1907436.
[101] L. Qie, Y. Lin, J. W. Connell, J. Xu, L. Dai, *Angew. Chem., Int. Ed.* **2017**, *56*, 6970.
[102] A. B. Kolomeisky, *J. Phys. Condens. Matter* **2013**, *25*, 463101.
[103] a) J. Howard, *Annu. Rev. Physiol.* **1996**, *58*, 703; b) G. Oster, H. Wang, *Trends Cell Biol.* **2003**, *13*, 114.
[104] a) N. Hirokawa, Y. Noda, Y. Tanaka, S. Niwa, *Nat. Rev. Mol. Cell Biol.* **2009**, *10*, 682; b) R. Cross, *Curr. Biol.* **1997**, *7*, R631.
[105] a) D. L. Coy, M. Wagenbach, J. Howard, *J. Biol. Chem.* **1999**, *274*, 3667; b) A. Yildiz, M. Tomishige, R. D. Vale, P. R. Selvin, *Science* **2004**, *303*, 676; c) K. Svoboda, C. F. Schmidt, B. J. Schnapp, S. M. Block, *Nature* **1993**, *365*, 721.
[106] N. J. Carter, R. Cross, *Nature* **2005**, *435*, 308.
[107] a) Y. Magariyama, S. Sugiyama, K. Muramoto, Y. Maekawa, I. Kawagishi, Y. Imae, S. Kudo, *Nature* **1994**, *371*, 752; b) R. Xue, Q. Ma, M. A. Baker, F. Bai, *Adv. Sci.* **2015**, *2*, 1500129.
[108] M. Meister, G. Lowe, H. C. Berg, *Cell* **1987**, *49*, 643.
[109] a) S. Kassem, T. van Leeuwen, A. S. Lubbe, M. R. Wilson, B. L. Feringa, D. A. Leigh, *Chem. Soc. Rev.* **2017**, *46*, 2592; b) S. Erbas-Cakmak, D. A. Leigh, C. T. McTernan, A. L. Nussbaumer, *Chem. Rev.* **2015**, *115*, 10081; c) K. Kinbara, T. Aida, *Chem. Rev.* **2005**, *105*, 1377; d) C. J. Bruns, J. F. Stoddart, in *The Nature of the Mechanical Bond: From Molecules To Machines*, John Wiley & Sons, Hoboken, NJ **2016**.
[110] P. L. Anelli, N. Spencer, J. F. Stoddart, *J. Am. Chem. Soc.* **1991**, *113*, 5131.
[111] R. A. Bissell, E. Córdova, A. E. Kaifer, J. F. Stoddart, *Nature* **1994**, *369*, 133.

[112] N. Koumura, R. W. Zijlstra, R. A. van Delden, N. Harada, B. L. Feringa, *Nature* **1999**, *401*, 152.
[113] J. Conyard, A. Cnossen, W. R. Browne, B. L. Feringa, S. R. Meech, *J. Am. Chem. Soc.* **2014**, *136*, 9692.
[114] a) J. Adler, *Annu. Rev. Biochem.* **1975**, *44*, 341; b) J. Adler, *Science* **1966**, *153*, 708 c) M. S. Kumar, P. Philominathan, *Biophys. Rev.* **2010**, *2*, 13.
[115] a) S. Childress, in *Mechanics of Swimming and Flying*, Vol. *2*, Cambridge University Press, Cambridge, UK **1981**; b) E. M. Purcell, *Proc. Natl. Acad. Sci.* **1997**, *94*, 11307; c) S. Chattopadhyay, R. Moldovan, C. Yeung, X. Wu, *Proc. Natl. Acad. Sci.* **2006**, *103*, 13712.
[116] a) A. Ghosh, P. Fischer, *Nano Lett.* **2009**, *9*, 2243; b) L. Zhang, J. J. Abbott, L. Dong, B. E. Kratochvil, D. Bell, B. J. Nelson, *Appl. Phys. Lett.* **2009**, *94*, 064107.
[117] J. Gibbs, P. Fischer, *Chem. Commun.* **2015**, *51*, 4192.
[118] D. Bray, in *Cell Movements: From Molecules to Motility*, Garland Science, New York, NY **2000**.
[119] a) E. A. Gillies, R. M. Cannon, R. B. Green, A. A. Pacey, *J. Fluid Mech.* **2009**, *625*, 445; b) C. Brennen, H. Winet, *Annu. Rev. Fluid Mech.* **1977**, *9*, 339; c) C. P. Lowe, *Philos. Trans. Roy. Soc. Lond. B: Biol. Sci.* **2003**, *358*, 1543; d) C. H. Wiggins, R. E. Goldstein, *Phys. Rev. Lett.* **1998**, *80*, 3879.
[120] R. Dreyfus, J. Baudry, M. L. Roper, M. Fermigier, H. A. Stone, J. Bibette, *Nature* **2005**, *437*, 862.
[121] E. M. Purcell, *Am. J. Phys.* **1977**, *45*, 3.
[122] a) W. Wang, W. Duan, S. Ahmed, T. E. Mallouk, A. Sen, *Nano Today* **2013**, *8*, 531; b) X. Ma, A. C. Hortelão, T. Patiño, S. Sánchez, *ACS Nano* **2016**, *10*, 9111.
[123] a) W. F. Paxton, K. C. Kistler, C. C. Olmeda, A. Sen, S. K. St. Angelo, Y. Cao, T. E. Mallouk, P. E. Lammert, V. H. Crespi, *J. Am. Chem. Soc.* **2004**, *126*, 13424; b) S. Fournier-Bidoz, A. C. Arsenault, I. Manners, G. A. Ozin, *Chem. Commun* **2005**, 441.
[124] W. Wang, T.-Y. Chiang, D. Velegol, T. E. Mallouk, *J. Am. Chem. Soc.* **2013**, *135*, 10557.
[125] a) J. L. Anderson, D. C. Prieve, *Separat. Purif. Methods* **1984**, *13*, 67; b) J. L. Anderson, *Annu. Rev. Fluid Mech.* **1989**, *21*, 61; c) Y. Hong, M. Diaz, U. M. Córdova-Figueroa, A. Sen, *Adv. Funct. Mater.* **2010**, *20*, 1568.
[126] C. Zhou, H. Zhang, J. Tang, W. Wang, *Langmuir* **2018**, *34*, 3289.
[127] R. A. Pavlick, S. Sengupta, T. McFadden, H. Zhang, A. Sen, *Angew. Chem., Int. Ed.* **2011**, *50*, 9374.
[128] a) M. Xuan, Z. Wu, J. Shao, L. Dai, T. Si, Q. He, *J. Am. Chem. Soc.* **2016**, *138*, 6492; b) H.-R. Jiang, N. Yoshinaga, M. Sano, *Phys. Rev. Lett.* **2010**, *105*, 268302.
[129] a) J. Li, I. Rozen, J. Wang, *ACS Nano* **2016**, *10*, 5619; b) Y. Mei, G. Huang, A. A. Solovev, E. B. Ureña, I. Mönch, F. Ding, T. Reindl, R. K. Fu, P. K. Chu, O. G. Schmidt, *Adv. Mater.* **2008**, *20*, 4085.
[130] L.L. Wang, L. Chen, J. Zhang, J. M. Duan, L. Wang, Z. H. Silber-Li, X. Zheng, H. H. Cui, *Langmuir* **2018**, *34*, 10426.
[131] a) P. Tierno, R. Golestanian, I. Pagonabarraga, F. Sagués, *Phys. Rev. Lett.* **2008**, *101*, 218304; b) C. E. Sing, L. Schmid, M. F. Schneider, T. Franke, A. Alexander-Katz, *Proc. Natl. Acad. Sci.* **2010**, *107*, 535; c) L. Zhang, T. Petit, Y. Lu, B. E. Kratochvil, K. E. Peyer, R. Pei, J. Lou, B. J. Nelson, *ACS Nano* **2010**, *4*, 6228.
[132] S. Palagi, A. G. Mark, S. Y. Reigh, K. Melde, T. Qiu, H. Zeng, C. Parmeggiani, D. Martella, A. Sanchez-Castillo, N. Kapernaum, *Nat. Mater.* **2016**, *15*, 647.
[133] T. Qiu, T.-C. Lee, A. G. Mark, K. I. Morozov, R. Münster, O. Mierka, S. Turek, A. M. Leshansky, P. Fischer, *Nat. Commun.* **2014**, *5*, 1.
[134] K. C. Neuman, S. M. Block, *Rev. Sci. Instrum.* **2004**, *75*, 2787.
[135] D. Fan, R. Cammarata, C. Chien, *Appl. Phys. Lett.* **2008**, *92*, 093115.
[136] I. De Vlaminck, C. Dekker, *Ann. Rev. Biophys.* **2012**, *41*, 453.
[137] A. Ozcelik, J. Rufo, F. Guo, Y. Gu, P. Li, J. Lata, T. J. Huang, *Nat. Methods* **2018**, *15*, 1021.
[138] J. E. Curtis, B. A. Koss, D. G. Grier, *Opt. Commun.* **2002**, *207*, 169.
[139] P. Y. Chiou, A. T. Ohta, M. C. Wu, *Nature* **2005**, *436*, 370.
[140] T. B. Jones, T. B. Jones, in *Electromechanics of Particles*, Cambridge University Press, Cambridge, UK **2005**.
[141] F. Guo, Z. Mao, Y. Chen, Z. Xie, J. P. Lata, P. Li, L. Ren, J. Liu, J. Yang, M. Dao, *Proc. Natl. Acad. Sci.* **2016**, *113*, 1522.
[142] a) A. Marzo, S. A. Seah, B. W. Drinkwater, D. R. Sahoo, B. Long, S. Subramanian, *Nat. Commun.* **2015**, *6*, 8661; b) K. Melde, A. G. Mark, T. Qiu, P. Fischer, *Nature* **2016**, *537*, 518.
[143] a) Z. Liang, D. Fan, *Sci. Adv.* **2018**, *4*, eaau0981; b) Z. Liang, D. Teal, D. E. Fan, *Nat. Commun.* **2019**, *10*, 1.
[144] V. Magdanz, S. Sanchez, O. G. Schmidt, *Adv. Mater.* **2013**, *25*, 6581.
[145] a) C. Chen, S. Tang, H. Teymourian, E. Karshalev, F. Zhang, J. Li, F. Mou, Y. Liang, J. Guan, J. Wang, *Angew. Chem.* **2018**, *130*, 8242; b) J. Guo, J. J. Gallegos, A. R. Tom, D. Fan, *ACS Nano* **2018**, *12*, 1179.
[146] G. Saper, H. Hess, *Chem. Rev.* **2019**, *120*, 288.
[147] H. Hess, V. Vogel, *Rev. Mol. Biotechnol.* **2001**, *82*, 67.
[148] D. Fan, Z. Yin, R. Cheong, F. Q. Zhu, R. C. Cammarata, C. Chien, A. Levchenko, *Nat. Nanotechnol.* **2010**, *5*, 545.
[149] T. G. Leong, C. L. Randall, B. R. Benson, N. Bassik, G. M. Stern, D. H. Gracias, *Proc. Natl. Acad. Sci.* **2009**, *106*, 703.
[150] Z. Wu, J. Troll, H.-H. Jeong, Q. Wei, M. Stang, F. Ziemssen, Z. Wang, M. Dong, S. Schnichels, T. Qiu, *Sci. Adv.* **2018**, *4*, eaat4388.
[151] S. Jeon, S. Kim, S. Ha, S. Lee, E. Kim, S. Y. Kim, S. H. Park, J. H. Jeon, S. W. Kim, C. Moon, *Sci. Robot.* **2019**, 4.
[152] M. Medina-Sánchez, L. Schwarz, A. K. Meyer, F. Hebenstreit, O. G. Schmidt, *Nano Lett.* **2016**, *16*, 555.
[153] Y. Alapan, U. Bozuyuk, P. Erkoc, A. C. Karacakol, M. Sitti, *Sci. Robot.* **2020**, 5.
[154] a) M. Z. Miskin, A. J. Cortese, K. Dorsey, E. P. Esposito, M. F. Reynolds, Q. Liu, M. Cao, D. A. Muller, P. L. McEuen, I. Cohen, *Nature* **2020**, *584*, 557; b) V. K. Bandari, Y. Nan, D. Karnaushenko, Y. Hong, B. Sun, F. Striggow, D. D. Karnaushenko, C. Becker, M. Faghih, M. Medina-Sánchez, *Nat. Electron.* **2020**, *3*, 172.

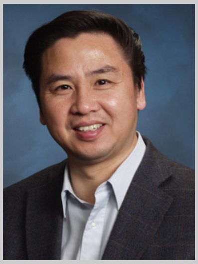

Liming Dai is an Australian Laureate Fellow, Scientia Professor, SHARP Professor and the Director of Australian Carbon Materials Centre at University of New South Wales, Sydney, Australia. Before joining UNSW, he spent 10 years with CSIRO (1992–2002) and was an associate professor of polymer engineering at the University of Akron (2002–2004), the Wright Brothers Institute Endowed Chair Professor of Nanomaterials at the University of Dayton (2004–2009), and the Kent Hale Smith Professor in the Department of Macromolecular Science and Engineering at Case Western Reserve University (2009–2019). He is a Fellow of the National Academy of Inventors (USA), Fellow of the American Institute for Medical and Biological Engineering, Fellow of the Royal Society of Chemistry, and Fellow of the European Academy of Sciences. His expertise covers the synthesis, functionalization, and device fabrication of conjugated polymers and carbon nanomaterials for energy-related and biomedical applications.

Donglei "Emma" Fan is an Associate Professor in the Department of Mechanical Engineering and a faculty member of the Materials Science and Engineering Program, Texas Materials Institute at The University of Texas at Austin. Her research focuses on intelligent micro/nanostructures, stimulus-responsive materials, and 3D hierarchical porous materials via understanding and exploiting fundamental materials science, physics, and chemistry. The efforts aim to address critical issues in micro/nanorobotics, soft robotics, biomedicine, and environment. Dr. Fan is an inventor of the patent awarded "Electric Tweezers" technique that can precisely manipulate longitudinal nanoparticles in suspension by combined AC and DC electric fields. Her team also discovered the effect of light-semiconductor-electric-field interaction for achieving unprecedented reconfigurable micro/nanomachines. Prof. Fan is a Fellow of the Royal Chemical Society (2021) and has being serving as an invited Japan Prize Official Nominator since 2017. In 2012, Prof. Fan received the National Science Foundation CAREER Award. Her work on the bottom-up assembling of artificial nanomotors was included in Science Year by Year, DK Smithsonian in 2017 and selected as the #3 of "10 discoveries that will shape the future in 2014" by the British Broadcasting Corporation (BBC) Focus magazine.

Arumugam Manthiram is the Cockrell Family Regents Chair in Engineering and the Director of Texas Materials Institute and Materials Science and Engineering Program at the University of Texas at Austin. His research is focused on the design and development of sustainable materials for batteries and fuel cells, with a focus on new low-cost, efficient materials, novel chemical synthesis and processing approaches, and a fundamental understanding of the structure-property-performance relationships of materials. He has authored 900 journal articles with 90 000 citations and an h-index of 148. He is a Web of Science Highly Cited Researcher every year since 2017. He has received numerous awards and recognitions, including the elected fellow of six professional societies. He delivered the 2019 Chemistry Nobel Prize Lecture in Stockholm on behalf of Professor John Goodenough.

Zhong Lin Wang is the Director of the Beijing Institute of Nanoenergy and Nanosystems, and Regents' Professor and Hightower Chair at Georgia Institute of Technology. Dr. Wang pioneered the nanogenerators field for distributed energy, self-powered sensors and large-scale blue energy. He coined the fields of piezotronics and piezo-phototronics for the third generation semiconductors. Among 100,000 scientists across all fields worldwide, Wang is ranked #3 in career scientific impact, #1 in Nanoscience, and #1 in Materials Science. His google scholar citation is over 328 000 with an h-index of over 276. Dr. Wang has received the Albert Einstein World Award of Science (2019); Diels-Planck lecture award (2019); ENI award in Energy Frontiers (2018); The James C. McGroddy Prize in New Materials from American Physical Society (2014); and MRS Medal from Materials Research Soci. (2011). Dr. Wang is the founding editor and chief editor of an international journal Nano Energy, which now has an impact factor of 17.88.